Self-Assembled Heterometallic Complexes by Incorporation of Calcium or Strontium Ion into a Manganese(II) 12-Metallacrown-3 Framework Supported by a Tripodal Ligand with Pyridine-Carboxylate Motifs: Stability in Their Manganese(III) Oxidized Form

Eric Gouré, Bertrand Gerey, Catalina N Astudillo, Jacques Pécaut, Selim Sirach, Florian Molton, Jérôme Fortage, Marie-Noëlle Collomb

Self-assembled Heterometallic Complexes by Incorporation of Calcium or Strontium ion into a Manganese(II) 12-Metallacrown-3 Framework Supported by a Tripodal Ligand with Pyridine-Carboxylate Motifs: Stability in their Manganese(III) Oxidized Form

Eric Gouré,[a] Bertrand Gerey,[a,b] Catalina N. Astudillo,[a] Jacques Pécaut,[b] Selim Sirach,[a] Florian Molton,[a] Jérôme Fortage [a] and Marie-Noëlle Collomb [a,*]

[a] Univ. Grenoble Alpes, CNRS, DCM, 38000 Grenoble, France

[b] Univ. Grenoble Alpes, CEA, CNRS, IRIG, SyMMES, 38000 Grenoble, France

Email address: marie-noelle.collomb@univ-grenoble-alpes.fr

Abstract

We report on the isolation of a new family of μ-carboxylato-bridged metallocrown (MC) compounds by self-assembly of the recently isolated hexadentate tris(2-pyridylmethyl)amine ligand $tpada^{2-}$ incorporating two carboxylate units with metal cations. Twelve-membered MCs of manganese of the type 12-MC-3, namely $[\{Mn^{II}(tpada)\}_3(M)(H_2O)_n]^{2+}$ (**Mn_3M**) (M = Mn^{2+} (n = 0), Ca^{2+} (n = 1) or Sr^{2+} (n = 2)), were structurally characterized. The metallamacrocycles connectivity consisting in three –[Mn-O-C-O]– repeating units is provided by one carboxylate unit of the three $tpada^{2-}$ ligands, while the second carboxylate coordinated a fourth cation in the central cavity of the MC, Mn^{2+} or an alkaline-earth metal, Ca^{2+} or Sr^{2+}. The **Mn_3Ca** and **$\{Mn_3Sr\}_2$** join the small family of heterometallic manganese-calcium complexes and even rarer manganese-strontium complexes as models of the OEC of photosystem II (PSII). A 8-MC-4 of strontium of the molecular wheel type with four –[Sr-O]– repeating unit was also isolated by self-assembly of the $tpada^{2-}$ ligand with Sr^{2+}. This complex, namely $[Sr(tpada)(OH_2)]_4$ (**Sr_4**), does not incorporate any cation in the central cavity but instead four water molecules coordinated to each Sr^{2+}. Electrochemical investigations coupled to UV-visible absorption and EPR spectroscopies as well as electrospray mass spectrometry reveal the stability of the 12-MC-3 tetranuclear structures in solution, both in the initial oxidation state, **Mn^{II}_3M**, as well as in the three-electrons oxidized state, **Mn^{III}_3M**. Indeed, the cyclic voltammogram of all these complexes exhibits three-successive reversible

oxidation waves between +0.5 and +0.9 V corresponding to the successive one-electron oxidation of the Mn(II) ion into Mn(III) of the three {Mn(tpada)} units constituting the ring, which are fully maintained after bulk electrolysis.

Introduction

Heterometallic manganese-calcium and manganese-strontium complexes are of special interest because of their relevance to the structure of the active center of the oxygen-evolving complex (OEC) of Photosystem II (PSII), an asymmetric oxo-bridged Mn_4CaO_5-cluster stabilized by six carboxylates ligands and one histidine.[1-4] Four water molecules directly also coordinated to the cluster (two to the Ca^{2+} ion and the other to the outer manganese) may act as substrates for dioxygen formation.[1, 5] Calcium is essential for the assembly and reassembly processes of the OEC as well as for the oxygen-evolving activity, although its role is not fully elucidated.[6-12] Regarding strontium, although this alkaline-earth metal is not present in the native enzyme, its comparable size and Lewis acidity make Sr^{2+} the only cation able to reproduce about half of the activity in a PSII from which Ca^{2+} has been removed.[13-16] Only few heterometallic manganese-calcium and manganese-strontium compounds have been isolated, and most examples have been published in the last ten years, reflecting a still largely unexplored area of research and also the synthetic difficulty to access such compounds.[1, 17-29] These complexes present a large variety of structures, topology and oxidation states, ranging from polymer to high nuclearity $Mn_{13}Ca_2$ clusters and only a few of them are close structural mimics of the OEC.[24, 28, 30-33] Among the synthetic Mn-Ca complexes, we have succeeded in the isolation of rare examples of carboxylate-bridged manganese(II)-calcium(II) complexes from the deprotonated tripodal tris(2-pyridylmethyl)amine hepta- and hexadentate ligands, $tpaa^{3-}$ and $tpada^{2-}$, incorporating respectively three and two pyridine-carboxylate units: the tetranuclear $[\{Mn^{II}(tpaa)\}_2\{Ca(OH_2)_5(\mu\text{-}OH_2)\}_2]^{2-}$ (**$Mn_2(tpaa)_2Ca_2(H_2O)_{12}$**) and the dinuclear $[Mn(tpada)ClCa(OH_2)_{2.67}(MeOH)_{2.33}]^-$ (**Mn(tpada)Ca(H_2O)$_3$**) (Figure 1). These complexes are potentially relevant for mimicking the first stages of the OEC assembly process.[34-35] In these complexes, the coordination of calcium is facilitated by the carboxylate functions incorporated in the periphery of the ligands framework. In **Mn(tpada)Ca(H_2O)$_3$**, the Mn^{2+} and Ca^{2+} ions are bridged *via* two $\mu_{1,1}$-carboxylato units, while in **$Mn_2(tpaa)_2Ca_2(H_2O)_{12}$** only one $\mu_{1,3}$-carboxylate bridge connects each Ca^{2+} ion to each Mn(II). The **Mn(tpada)Ca(H_2O)$_3$** complex was obtained by displacement of the Ca^{2+} ion in the neutral dinuclear calcium complex, $[Ca(tpada)(OH_2)_2]_2$ (**$Ca_2(tpada)_2(H_2O)_4$**), with Mn^{2+} (Figure 1).

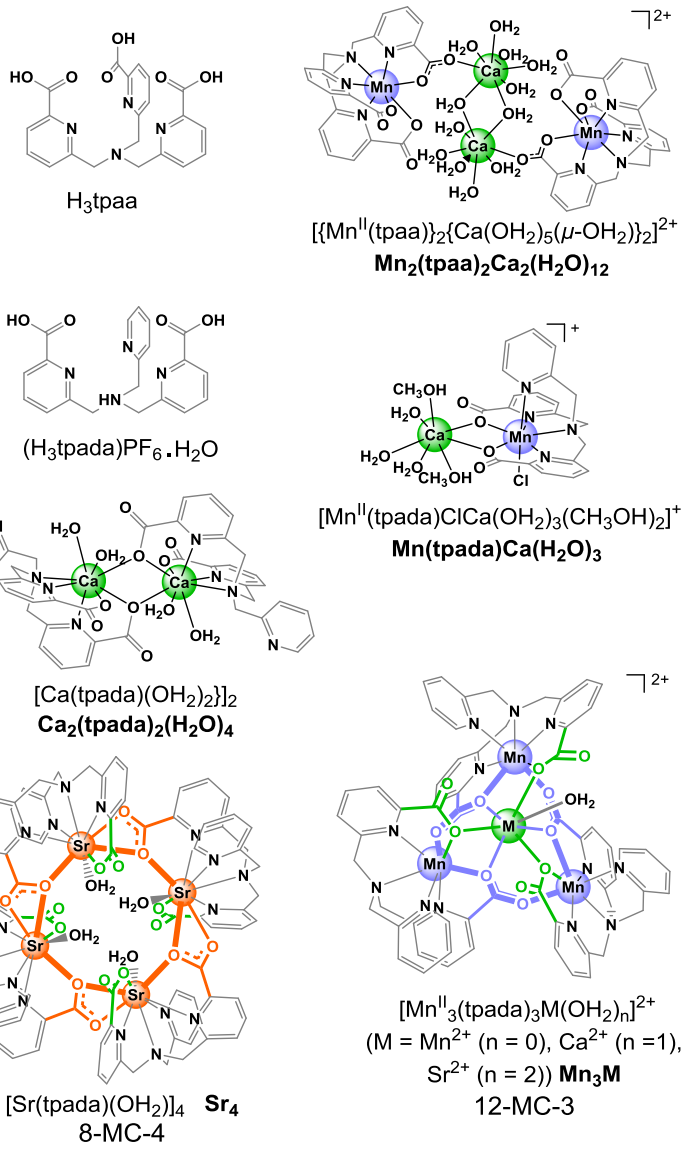

Figure 1: Structures of the Mn-Ca and Ca complexes previously isolated by our group[35] and of the 8-MC-4 and 12-MC-3 complexes isolated in this work from the carboxylate-functionalized tpaa^{3-} and tpada^{2-} tripodal ligands (Adapted from Ref. [35], with permission from the Royal Society of Chemistry, Copyright 2015).

On the other hand, multidentate ligands containing one or more carboxylate moieties can also lead to original self-assembled metallamacrocyclic-type structures, also called metallacrowns (MCs), able to trap, in some cases, a cation in their cavity.[36] In such complexes, the metals forming the macrocycle are linked either with $\mu_{1,3}$- or $\mu_{1,1}$-carboxylato bridges of the ancillary ligand corresponding to –[M-O-C-O]– or [M-O]– repeat unit. Among the numerous examples of metallamacrocycles, metallacrowns based on such μ-carboxylato bridges are not common.[37-41] Four examples of the type 12-MC-3, *i. e.* a 12-membered ring comprising 3 repeating units of –[M-O-C-O]– have been isolated from the deprotonated monocarboxylate tripodal ligand bpg$^-$ (bis(2-picolyl)glycine) with zinc(II) or iron(II) (Figure

2(A)). The three metal centers are linked by a $\mu_{1,3}$-carboxylato of the tripodal ligand. Two of the iron metallacrowns described have encapsulated a Fe^{2+} central cation which is linked to the peripheral ions by three oxygen atoms of the ring and by three additional $\mu_{1,3}$-acetato[39] or $\mu_{1,3}$-benzoato[38] bridges (Figure 2(A(c))). The others examples of μ-carboxylato bridges metallacrowns, of higher nuclearity, have been described using copper(II) salts from triscarboxylate ligands derived from glycine.[40-41]

Considering metallacrowns with manganese, a series of 12-MC-4 of Mn(III) were obtained with the deprotonated multidentate salicylhydroxamic acid ligand (shi^{3-}) that does not contain carboxylate units (Figure 2(B)).[36, 42-48] In this case, the four Mn(III) ions are linked by the N and O atoms of the oximate group from the shi^{3-} ligand forming a twelve-membered $\{M\text{-}O\text{-}N\}_4$ MC that can host a large variety of cations in their cavity, including Mn^{2+}, Li^{+}, Na^{+}, lanthanides but also Ca^{2+}. Similarly to the iron MC mentioned above, the central cation is coordinated either by oxygen atoms of the ring and by additional acetates or benzoates that bridge with the Mn(III) ions of the macrocycle.

In the present study, we report on the isolation and the structural characterization of a new family of manganese(II) MCs, based on the –[Mn-O-C-O]– repeating motif, from the recently isolated hexadentate $tpada^{2-}$ ligand.[35] The schematic structure of the complexes of general formula, $[\{Mn^{II}(tpada)\}_3M^{II}(H_2O)_n]^{2+}$ (**Mn_3M**) with M = Mn^{2+} (n = 0), Ca^{2+} (n = 1) or Sr^{2+} (n = 2), is shown in Figure 1. These self-assembled 12-MC-3 manganese(II) MCs forming a twelve-membered ring with three Mn^{2+} centers bridged by $\mu_{1,3}$-carboxylato, encapsulate a fourth cation in their central cavity. The first crystallographic structure with a good resolution was obtained with the central unit occupied with a Mn^{2+} ion. We then investigated the possibility of replacing this central cation with redox-innocent cations such as calcium and strontium, in order to expand the family of models of the OEC center of PSII. We also explore the molecular architecture that arises upon the self-assembly of the $tpada^{2-}$ ligand with only Sr^{2+}, with the objective of identifying the coordination mode of strontium with this ligand in comparison to calcium,[1] in particular its affinity for aqua ligands. Another type of MC was obtained of the type molecular wheel, namely $[Sr(tpada)(OH_2)]_4$ (**Sr4**) in the form of a 8-MC-4, with four Sr^{2+} ions bridged *via* a $\mu_{1,1}$-carboxylato bridge, without any cation in the central cavity.

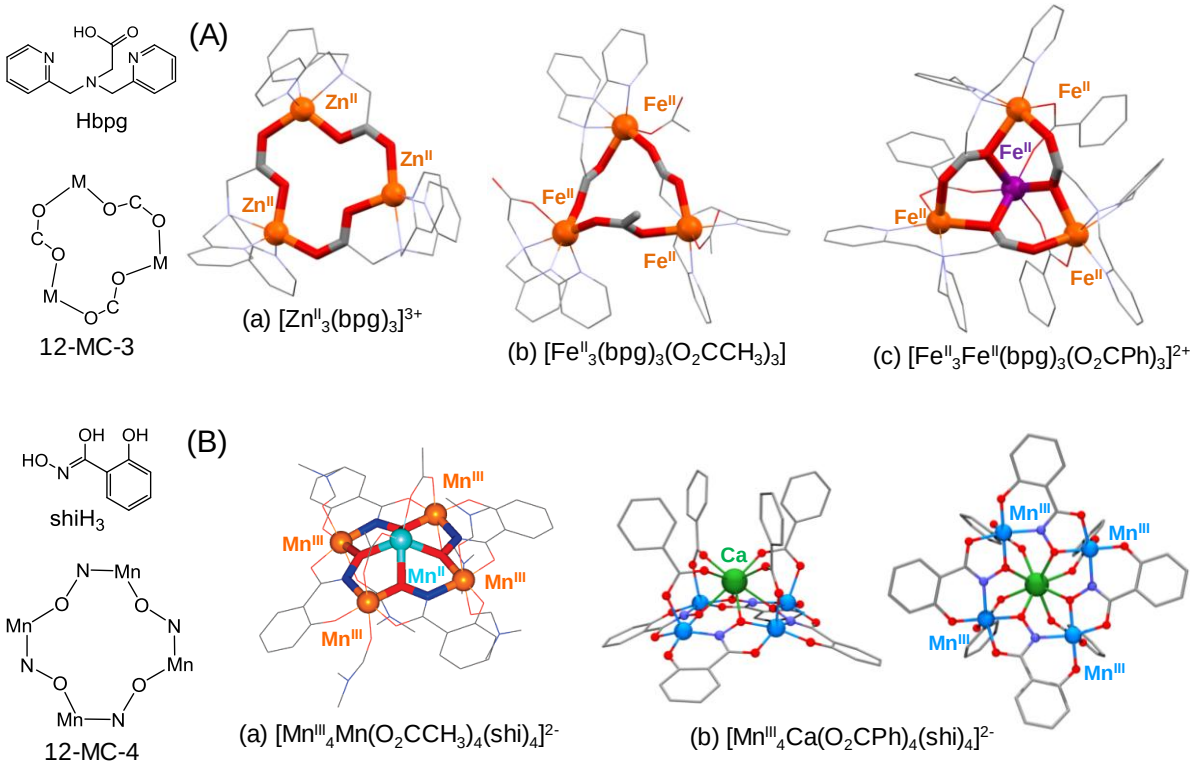

Figure 2: Crystallographic structures of the (A) 12-MC-3 complexes of Zn^{2+} (a) and Fe^{2+} (b-c) with the bpg^- ligand providing the O-C-O bridging moiety. A Fe^{2+} is encapsulated within the central cavity of the Fe^{2+} MC ring (c). (B) 12-MC-4 complexes of Mn^{3+} with the shi^{3-} ligand providing the O-N bridging moiety encapsulating a Mn^{2+} ion (a) and a Ca^{2+} ion (two views) (b) within the central cavity. Schematic representations of the corresponding ligands and atom connectivity of the metallamacrocycle.

In this article, we will first discuss the synthesis and the X-ray structures of the **Mn_3M** and **Sr_4** MC complexes. We will then report on solution studies in organic solvent (CH_3CN) by electrospray mass spectrometry and electrochemistry in combination with UV-visible absorption and EPR spectroscopy of the **Mn_3M** complexes. The aim of these solution studies was to establish the stability of the tetranuclear MC structure of these complexes in solution and to investigate their redox properties. Only few studies in solution have been conducted on metallamacrocyclic complexes and to the best of our knowledge, the stability in solution and the redox properties of the family of μ-carboxylato bridged MCs have never been investigated.

Results and discussion

Synthesis and crystal structures of the complexes Mn_3M (M = Mn^{2+}, Ca^{2+}or Sr^{2+})

The first metallamacrocyclic 12-MC-3 complex of our series, in which three {Mn(tpada)} units are bridged by $\mu_{1,3}$-carboxylate O atoms, was obtained with the central cavity occupied by a Mn^{2+} cation. This result prompted us to investigate the insertion of other

cations in the central cavity such as divalent Ca^{2+} and Sr^{2+} ions in order to obtain new heteronuclear MC complexes. To access these complexes, the ligand $(H_3tpada)PF_6 \cdot H_2O$ was first fully deprotonated in methanol by addition of a base (Scheme 1). The tetranuclear MC with a Mn^{2+} in the central cavity (**Mn_3Mn**) was then obtained by the spontaneous self-assembly of the $tpada^{2-}$ ligand with 1.4 equivalents of manganese(II) acetate in methanol at room temperature (Scheme 1(a)). Only one equivalent of manganese(II) acetate per $tpada^{2-}$ was used for the heteronuclear MCs, **Mn_3Ca** and **Mn_3Sr**, followed by the addition of an excess (1 to 1.3 equivalents per ligand) of the second metal salt (M = Ca^{2+}or Sr^{2+}) in acetonitrile or in acetonitrile/water (Scheme 1(b, c)). The three complexes were isolated in good yields (from 88 to 97 %) as microcrystalline pale yellow powders by partial evaporation of the solvents. The **Mn_3Mn** and **Mn_3Ca** crystallized in their tetranuclear forms, while two **Mn_3Sr** units associate *via* two bridging $\mu_{1,3}$-carboxylates from $tpada^{2-}$ ligands and two bridging water molecules leading to the formation of the octanuclear **$\{Mn_3Sr\}_2$**$(PF_6)_4$ compound (Scheme 1(c)).

Single crystals of $[\{Mn^{II}(tpada)\}_3Ca(OH_2)](PF_6)_2 \cdot 1.75CH_3CO_2C_2H_5 \cdot 0.25CH_3CN$ (**Mn_3Ca**$(PF_6)_2 \cdot 1.75EtOAc \cdot 0.25CH_3CN$) and $[\{Mn^{II}(tpada)\}_3Sr(\mu\text{-}OH_2)]_2(PF_6)_4 \cdot 2CH_3OH \cdot 1.5AcOEt \cdot 0.5H_2O$ (**$\{Mn_3Sr\}_2$**$(PF_6)_4 \cdot 2CH_3OH \cdot 1.5AcOEt \cdot 0.5H_2O$) were formed by slow diffusion of ethyl acetate or diethyl ether into acetonitrile solution of the respective compound. The crystallographic data of the complexes are summarized in Table S1 and selected bond lengths and angles in Tables S2-S11. By contrast, single crystals suitable for X-ray diffraction analysis of the manganese derivative, $[\{Mn^{II}(tpada)\}_3Mn^{II}](ClO_4)_2 \cdot 2CH_3CN$ (**Mn_3Mn**$(ClO_4)_2 \cdot 2CH_3CN$), were only obtained by using perchlorate as counter ions. An excess of $Li(ClO_4)$ was added to the acetonitrile solution of the **Mn_3Ca**$(PF_6)_2$ complex for the crystallization step (see Supporting Information). Figure 3 displays the crystallographic structures of the **Mn_3M** complexes. For all complexes, charge considerations require that the three $tpada^{2-}$ ligands are deprotonated. The structure of the **Mn_3Mn** cation consists of three bridged $\{Mn^{II}(tpada)\}$ unit surrounding a central Mn^{2+} cation which is coordinated to six carboxylate O atoms. The three manganese are bridged to each other by $\mu_{1,3}$-carboxylato bridges from one of the two carboxylate groups of the $tpada^{2-}$ ligands forming a twelve-membered metallamacrocycle of the MC type with a $–[Mn^{II}\text{-}O\text{-}C\text{-}O]–$ repeating unit (Scheme 1).

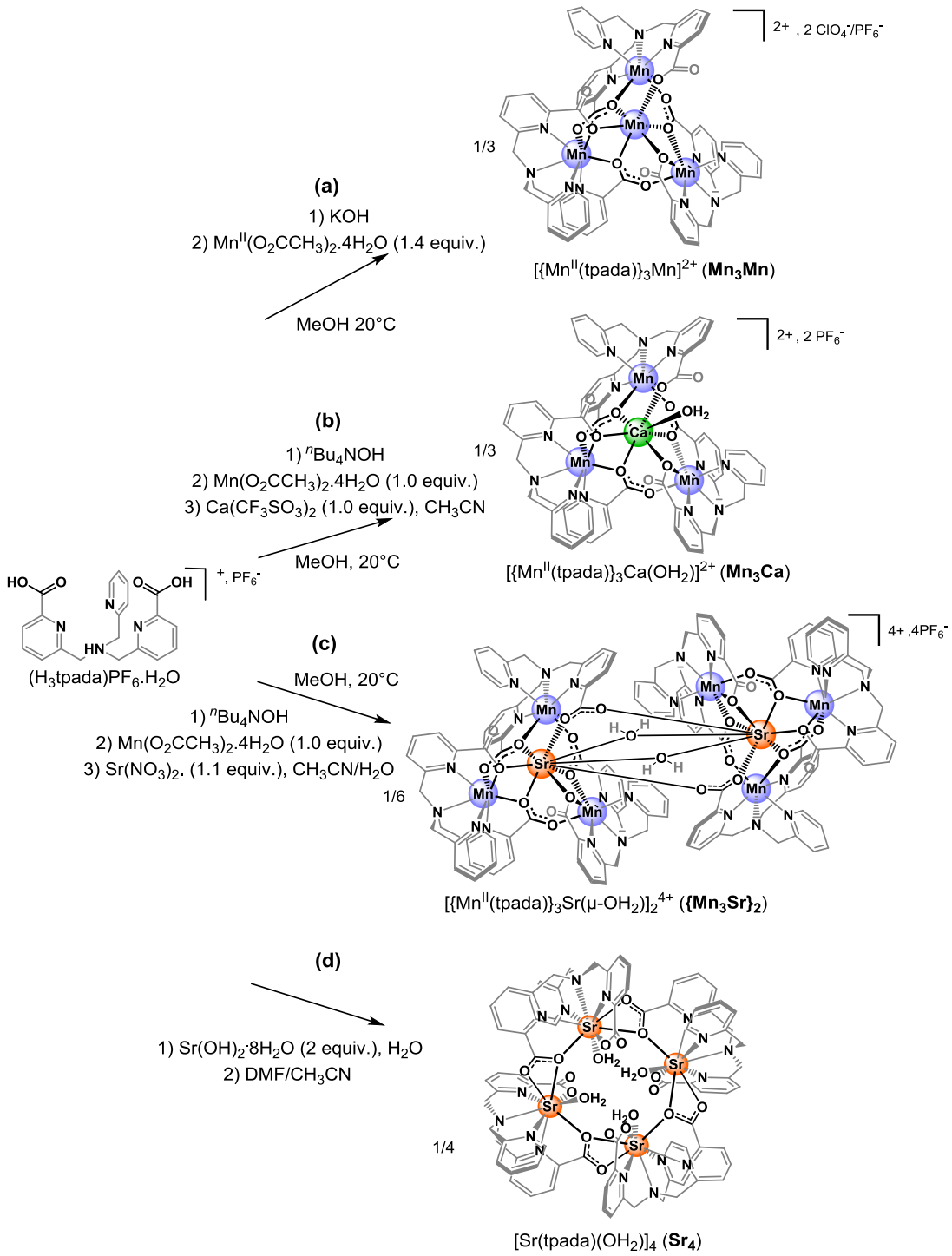

Scheme 1. Synthetic routes for the homo- and heteronuclear 12-MC-3 and 8-MC-4 complexes.

This arrangement generates a cavity at the center of the structure of six oxygen atoms of the tpada^{2-} ligands (three of them do not participate in the macrocycle) allowing the molecule to host a fourth metal center. The Mn^{2+} cation present in the central cavity is thus coordinated to the six O donors in a distorted octahedral geometry, and linked to each manganese(II) of the {Mn^{II}(tpada)} units *via* two $\mu_{1,1}$-carboxylato bridges (Scheme 1 and Figure 3(a)). The

presumed strong coordination in the central cavity possibly explains that we did not succeed in isolation a metallamacrocycle without any cation within the central cavity. In other words, the stability of the MC structure is probably reinforced by the presence of the central cation.

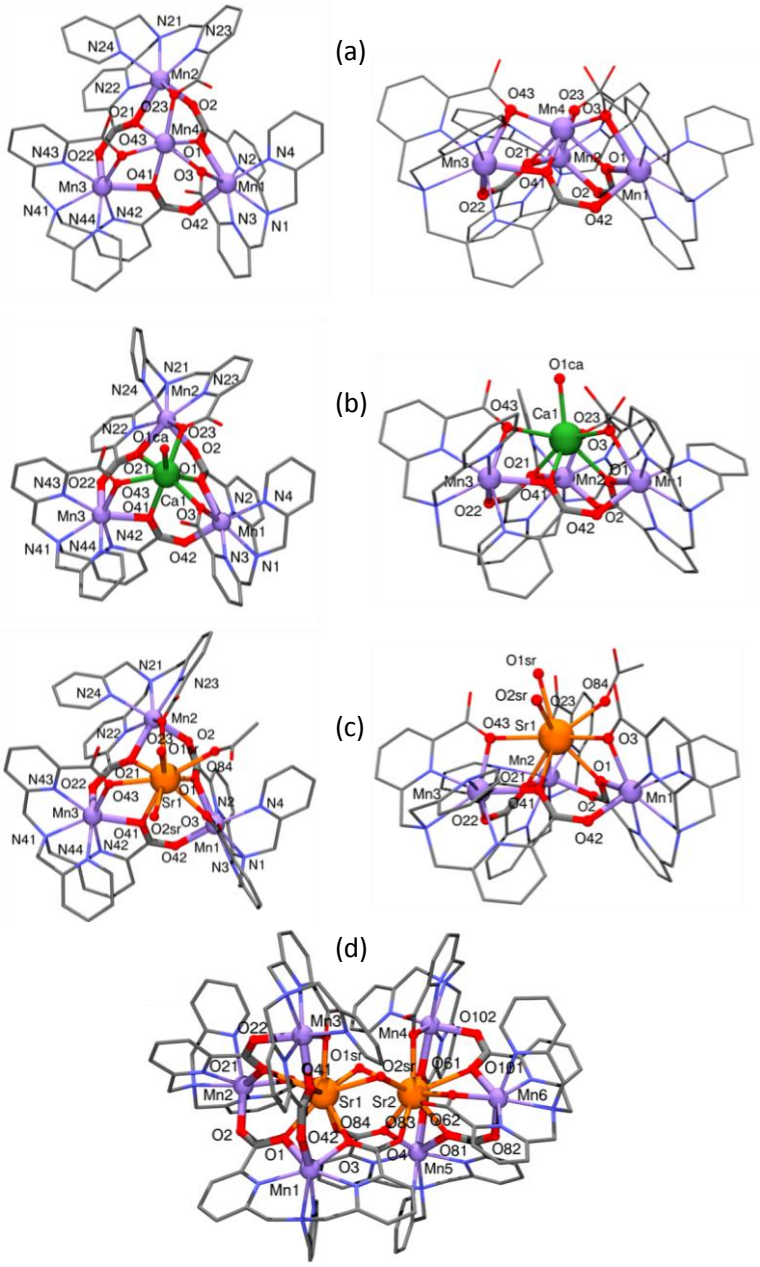

Figure 3. Representations of the crystallographic structures obtained by X-ray diffraction of the cationic forms of the complexes **Mn_3Mn** (a), **Mn_3Ca** (b), **Mn_3Sr** (c) and **$\{Mn^{II}_3Sr\}_2$** (d). View along the pseudo axis of symmetry 3 (left) and view of the metallamacrocycle cavity (right). Hydrogen atoms have been omitted for clarity.

Figure 4 displays the coordination sphere of one of the three $\{Mn^{II}(tpada)\}$ units, and of the Mn^{2+} present in the cavity. In each $\{Mn^{II}(tpada)\}$ unit, the Mn^{2+} cation is coordinated to all six donor atoms of the $tpada^{2-}$ ligand and to one carboxylate O atom from the $tpada^{2-}$ ligand of a neighboring {Mn(tpada)} unit, in an approximately pentagonal bipyramidal geometry (Figures 3(a) and 4(b)). The N-O pairs of the two pyridine-carboxylate $tpada^{2-}$ ligand and the

N tertiary (N_{tert}) amine are close to coplanar with the Mn^{2+} ion, while the axial positions are occupied by the pyridine N atom and the bridging carboxylate O atom (Figure 4(b)). This geometry around each Mn^{2+} ion is very similar to that found in the binuclear **Mn(tpada)Ca(H_2O)$_3$** except that instead of a bridging carboxylate O atom, a chloride ion occupies the axial position (Figure 1).[35] The Mn-N_{tert} bonds are also significantly longer than the Mn-N_{py} and Mn-O bonds (average 2.43(1) Å, v*ersus* 2.24(1) Å and 2.24(3) Å (Table S2)) due to the steric constraints imposed by the ligand, but consistent with all Mn(II) centers.[35] The Mn•••Mn distances and intermetallic angles within the macrocycle show that the three Mn^{2+} ions form an essentially isosceles triangle (Table S9). We can therefore consider that a pseudo axis of symmetry 3 passes through the center of the cavity.

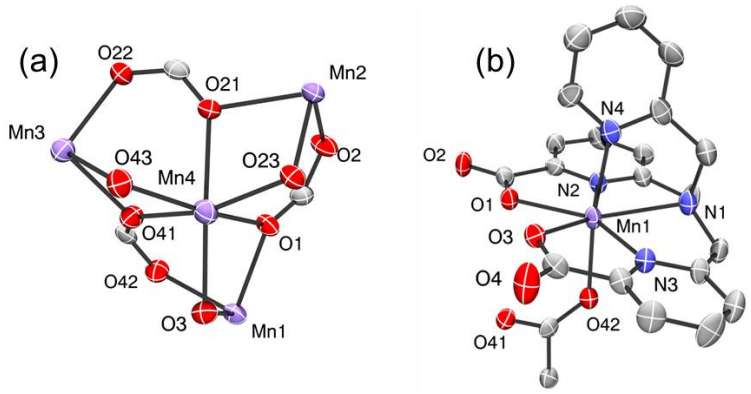

Figure 4. ORTEP drawing with thermal ellipsoids at 50% probability of the O_6 coordination sphere of the Mn^{2+} ion present in the central cavity of **Mn_3Mn** (a) and of one of the three {Mn^{II}(tpada)} unit of **Mn_3Mn** (b). Hydrogen atoms have been omitted for clarity.

The macrocyclic structures of the heteronuclear **Mn_3Ca** and **{Mn_3Sr}$_2$** compounds are similar to that of **Mn_3Mn**, and we will therefore only discuss on the differences induced by the substitution of the Mn^{2+} ion of the central cavity by the redox-innocent Ca^{2+} and Sr^{2+} cations. In **Mn_3Mn**, the central Mn^{2+} cation is arranged in Δ stereochemical conformation, while in the heteronuclear clusters, Ca^{2+} and Sr^{2+} are present in the two conformations, Δ and Λ.

The Mn-O/N distances in the {Mn(tpada)} units are rather similar for the different complexes, although with strontium these are slightly longer: for **Mn_3Mn**, **Mn_3Ca** and **{Mn_3Sr}$_2$** the Mn-N_{tert} average distances are respectively 2.434(6), 2.459(10) and 2.491(17) Å and those of Mn-N_{py}/O_{COO}- of 2.24(3), 2.23(4) and 2.25(6) Å, respectively (Table S10). On the other hand, the distances between the Mn^{2+} ions and the central M^{2+} cation (Mn•••M distances) (Table S10) as well as the distances between the M^{2+} and the plane formed by the three Mn^{2+} ions (1.255(1) (**Mn_3Mn**) < 1.562(1) (**Mn_3Ca**) < 1.978(21) Å (**{Mn_3Sr}$_2$**)) increase significantly with the ionic radius of the M^{2+} cation, *i. e.* from manganese to strontium (83 μm (Mn^{2+})

<100 μm (Ca^{2+}) <118 μm (Sr^{2+})).[49] In other words, the larger the size of the cation, the greater its distance from the plane formed by the three manganese ions. This is also reflected by the bond distances of the central M^{2+} cation that significantly increase with the size of the cation (average distances of M-O_{COO}-: 2.20 (7) Å (Mn^{2+}), 2.41 (4) Å (Ca^{2+}) and 2.65 (10) Å (Sr^{2+}) (Table S11). Besides, the similarity of the Mn···Mn distances for **Mn_3Ca** and **{Mn_3Sr}$_2$**, although slightly higher than those of **Mn_3Mn** (Table S9), indicates that beyond calcium, the structural change of the metallamacrocycle to accommodate the strontium does not simply involve an increase of the Mn···Mn distances, but by a shift of the Sr^{2+} cation away from the plane formed by the three Mn^{2+} ions.

Finally, regarding the coordination of the central cation, the calcium, capped with a water molecule, is heptacoordinated (Figure 3(c)), adopting an antiprism distorted geometry with a capped face. On the other hand, the strontium is coordinated by two water molecules which act as bridges with the strontium of the second **Mn_3Sr** tetranuclear unit (Figure 3(d)). The coordination sphere of the Sr^{2+} ion is also supplemented by a O donor from the carboxylate of the neighboring **Mn_3Sr** tetranuclear unit resulting in two additional $\mu_{1,3}$-carboxylato bridges between the two Sr^{2+} cations (Scheme 1(c) and Figure 3(d)). The strontium is thus nonacoordinated as in the $[Sr(tpada)(OH_2)]_4$ (**Sr_4**) complex (see below), in a geometry however difficult to determine. Nonacoordinated strontium ions with only oxygen in their coordination sphere are also observed in the Mn-Sr heteronuclear $[LMn^{IV}{}_3SrO_4(OAc)_3(DMF)]_2$ cluster isolated by the Agapie group.[50] The two cubanoid units $\{Mn^{IV}{}_3SrO_4\}_2$ that constitute this complex are also associated by two bridging $\mu_{1,1}$-carboxylato and two bridging DMF molecules (DMF = N,N-dimethylformamide).

Synthesis and crystal structures of the Sr_4 complex

We have also explored the molecular architecture that arises upon the self-assembly of the $tpada^{2-}$ ligand with Sr^{2+}. By reacting the $(H_3tpada)PF_6 \cdot H_2O$ ligand with two equivalents of $Sr(OH)_2 \cdot 8H_2O$ in water, another type of MC was obtained having four –[Sr-O]– repeating units, and without any cation in the central cavity (Scheme 1(d) and Figure 5). The crystallographic data and selected bond distances and angles are given in Tables S12-S14. The structure of the neutral $[Sr(tpada)(OH_2)]_4 \cdot 8CH_3CN \cdot 2H_2O$ (**Sr_4**$\cdot 8CH_3CN \cdot 2H_2O$) complex consists of four neutral $\{Sr(tpada)(OH_2)\}$ units in which each Sr^{2+} cation is bridged to its neighbors by a bidentate carboxylate ligand of a neighbouring ligand, forming an eight-membered metallamacrocycle in the form of a 8-MC-4, which is, to our knowledge, the first strontium-based molecular metallamacrocycle of the type molecular wheel.

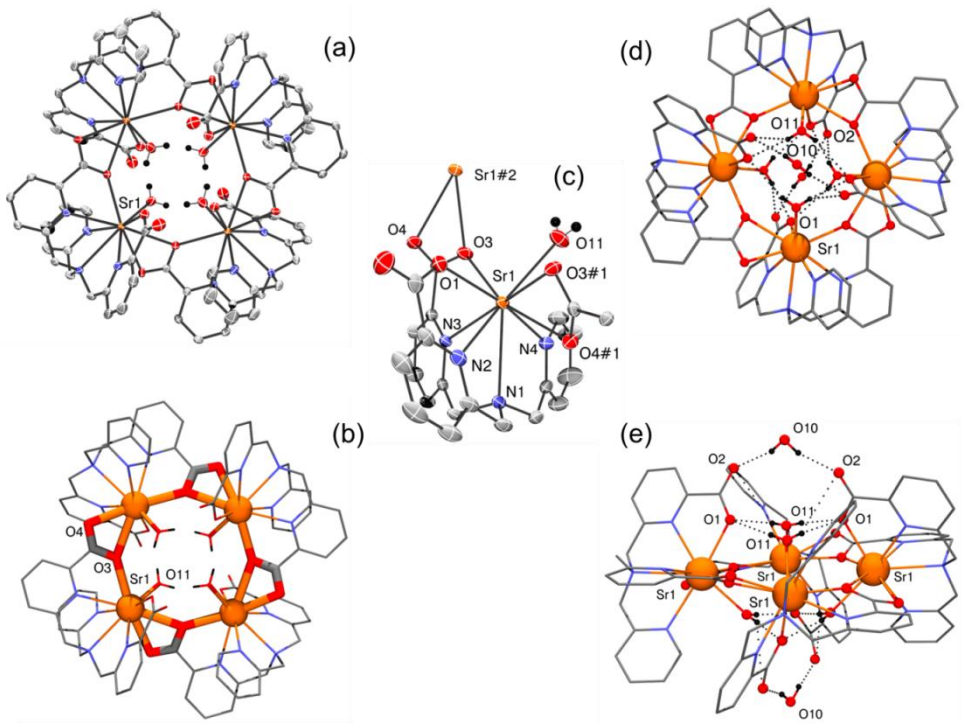

Figure 5. ORTEP drawings with thermal ellipsoids at 50% probability of the tetranuclear 8-MC-4 $[Sr(tpada)(OH_2)]_4$ (**Sr$_4$**•$8CH_3CN$•$2H_2O$); view along the axis of symmetry -4 (a) and (b); view of the monomeric unit $\{Sr(tpada)(OH_2)\}$ linked to one neighboring strontium (c) and views of the hydrogen bond network perpendicular (d) and parallel (e) of the macrocycle plan. Only relevant hydrogens are shown for clarity.

Each Sr^{2+} ion is thus separated from its neighbour by only an O atom of a carboxylate. The metallamacrocycle is plane and the four Sr^{2+} ions form a square. Each Sr^{2+} cation is coordinated to nine donor atoms in an N_4O_5 coordination sphere, six of the deprotonated $tpada^{2-}$ ligand, one O atom from an aqua ligand and two O atoms from a bidentate carboxylate κ^2O^1,O^3 from a $tpada^{2-}$ ligand of a neighbouring $\{Sr(tpada)(OH_2)\}$ unit. The geometry around each Sr^{2+} can be described as a rectangular prism having a capped face, the O(1), O(3), O(3)#1 and O(11) atoms forming the inner face, while the O(4)#1, N(2), N(3) and N(4) atoms forming the upper face capped by the atom N(1) from the tertiary amine (Figure 5(c)). Regarding the Sr-O/N bond distances, the average distances Sr-N_{py} and Sr-O (excluding the distance Sr-O(3)#1) are of 2.748(11) Å and 2.592(18) Å respectively, and two distances are significantly longer compared to the others: the Sr-N_{tert} distance of 2.9132(18) Å, and the Sr-O(3)#1 distance formed with a neighbouring carboxylate of 2.7550(15) Å, *i.e.* + 0.15 Å compared to the other Sr-O distances (Table S13). These distances are longer than those observed in the $\{Ca(tpada)(OH_2)\}$ units of the neutral dinuclear $[Ca(tpada)(OH_2)_2]_2$ which are actually longer than those of the $\{Mn(tpada)\}$ units in the **Mn$_3$M** complexes, in accordance

with the size of the respective cation (Sr^{2+} > Ca^{2+} > Mn^{2+}) (see above). The aqua ligand of each strontium is in *trans* position with respect to the two neighbouring aqua ligands and in *cis* position with respect to the aqua ligand of the strontium facing it; this distribution corresponding to a -4 axis of symmetry. Thus two aqua ligands are located respectively above and below the plane formed by the metallamacrocycle. These aqua ligands are involved in several intra- and inter-molecular hydrogen bonds (Figure 5(d-e) and Table S14).

Electrospray Ionization (ESI) Mass Spectrometry.

To evaluate the structural integrity of the **Mn_3M** complexes in solution, electrospray mass spectrometry and electrochemical experiments have been carried out in CH_3CN.

The positive mode ESI spectra of **Mn_3M** obtained in CH_3CN solution are shown in Figure S1. For all complexes, the two main peaks observed correspond to the di- and mono-charged species $\{Mn_3(tpada)_3M\}^{2+}$ and $[\{Mn_3(tpada)_3M\}(PF_6)]^{+}$. The most intense ones corresponding to the dicationic species are located at *m/z* 674.1, 666.6 and 690.7 for $\{Mn_3(tpada)_3Mn\}^{2+}$, $\{Mn_3(tpada)_3Ca\}^{2+}$ and $\{Mn_3(tpada)_3Sr\}^{2+}$ respectively, while the lower intensity peaks belonging to the monocationic species are detected at *m/z* 1493.1, 1478.1 and 1526.0 for $[(Mn_3(tpada)_3Mn\}(PF_6)]^{+}$, $\{Mn_3(tpada)_3Ca\}(PF_6)]^{+}$ and $[\{Mn_3(tpada)_3Sr\}(PF_6)]^{+}$, respectively. These assignments are confirmed by simulations of the isotopic massifs which reproduce the experimental isotopic distributions (Figure S1, insert). From these results, it is possible to conclude that to the MC tetranuclear structure of the **Mn_3M** complexes are maintained in acetonitrile solution. However, the water molecule(s) coordinated to the Ca^{2+} and Sr^{2+} are not retained in the mass spectrometry conditions. Furthermore, the dimeric structure of the **$\{Mn^{II}_3Sr\}_2$** complex is not conserved under mass spectrometry conditions since the only detected species correspond to the tetranuclear **Mn^{II}_3Sr** unit.

To determine the fragmentation mode of such MC structure and evaluate its stability under severe ionization, an MS^2 analysis was carried out on the dication $\{Mn_3(tpada)_3Ca\}^{2+}$ at *m/z* 666.6. The MS^2 spectrum reveals the formation of two dicationic peaks at *m/z* 451.0 and 620.1 (Figure S1(D)). The *m/z* 451.0 species corresponds to the trinuclear $\{Mn_2(tpada)_2Ca\}^{2+}$ resulting from the loss of a monomeric unit {Mn(tpada)}. The second fragment, detected at *m/z* 620.1, originates from the fragmentation of one $tpada^{2-}$ ligand at the methyl level of the picoline (L'), $\{Mn^{II}_2(tpada)_2L'Ca\}^{2+}$. This fragmentation releases a picolyl radical and generate a rearrangement at the level of the tertiary nitrogen, forming a double bond with the methylene carbon of one of the two picolinates and accompanied by the loss of a proton.

These two fragments attest to the high stability of the **Mn_3Ca** cluster and the strong coordination of the encapsulated dication since despite the fragmentation of one of the ancillary $tpada^{2-}$ ligand and the modification of the metallamacrocycle structure by the loss of a {Mn(tpada) unit, the calcium remains coordinated. These studies confirm the stability of the MC structures in CH_3CN solution even under severe ionization and that the alkaline-earth cations remain coordinated in the metallamacrocycle cavity in solution.

Electrochemical and spectroscopic properties of Mn_3M in CH_3CN.

The electrochemical properties of the **Mn_3M** complexes have been investigated in CH_3CN under argon (Figures 6 and S2-S3). The cyclic voltammograms (CV) of all complexes exhibit three successive reversible oxidation waves located between +0.5 and +0.9 V (Table S15) assigned to the successive oxidation of the three Mn(II) ions into Mn(III) of the $\{Mn^{II}(tpada)\}$ units which forms the macrocycle. No other oxidation event is observed in the region of positive potentials when scanning up to +1.8 V. The presence of three one-electron redox processes, close in potential ($\Delta E_{1/2}$ = 130 - 170 mV) (Table S15), instead of a single three-electron wave, is the result of Coulombic interactions between the three electroactive centers.[51-53] Therefore, the oxidation of one Mn(II) into Mn(III) increases the positive field around its neighbors, altering the potential of those neighbors. In addition, the potential values of the reversible waves slightly differ according to the complexes. For example, considering the first reversible oxidation wave, the **Mn_3Mn** complex ($E_{1/2}$ = +0.62 V) is slightly more difficult to oxidize than complexes with calcium and strontium ions, **Mn_3Ca** and **$\{Mn_3Sr_2$**, which are very close in potential ($E_{1/2}$ = +0.57 and 0.58 V, respectively). Even if the influence of the nature of M^{n+} cation inserted in the cavity on the redox potential of the Mn(II) ions forming the metallamacrocycle is very weak, it is consistent with its preservation in the MC cavity. In comparison, a large positive shift of more than 1 V has been observed in the case of the Agapie's series of isostructural cubane clusters $[Mn^{IV}{}_3MO_4(L^6)(O_2CMe)_3(DMF)]^+$ for the Mn derivative compared to the Ca or Sr derivatives for which the potential are essentially the same ($E_{1/2}$ values of the $[MMn^{IV}{}_3O_4]/[MMn^{IV}{}_2Mn^{III}{}_2O_4]$ couples of +290 mV for M = Mn^{3+} and -940 mV *vs* Fc/Fc^+ for M = Ca^{2+} or Sr^{2+}).[50, 54] The large difference in potentials observed in this series of complexes, can be explain by the fact that all metal ions are strongly magnetically coupled through oxo bridges. It is worth noting that the oxidation process of the central Mn(II) ion in the **Mn_3Mn** complex is not accessible in the solvent electroactivity domain (no signal up to +1.8 V). This Mn^{2+} center is very depleted in electrons after the three

successive oxidations of the Mn^{2+} ions of the macrocycle, and therefore very difficult to oxidize.

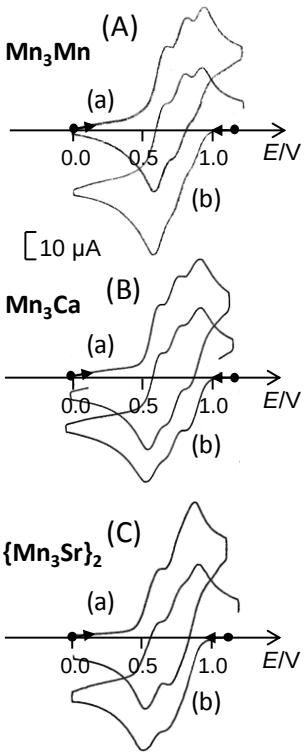

Figure 6: Cyclic voltammograms in CH_3CN, 0.1 M $[Bu_4N]ClO_4$ at a platinum electrode (υ = 100 mV s^{-1}) of solutions of (A) **Mn_3M** (0.64 mM), (B) **Mn_3Ca** (0.57 mM) and (C) **{Mn_3Sr}$_2$** (0.33 mM): (a) initial solutions and (b) after exhaustive oxidation at 1.20 V. Potentials are referenced to $Ag/AgNO_3$ (10 mM).

In the region of the negative potentials, a series of reversible systems very close in potential ($\Delta E_{1/2}$ of about 100 mV) are also detected between -2.0 and -2.7 V (Figures S2-S3 for CVs recorded on carbon electrode). These ligand-centered reduction processes are reasonably assigned to the successive monoelectronic reduction of the pyridine-carboxylate units of the $tpada^{2-}$ ligands. Similarly to the reversible oxidation systems, potential shifts are found on these reduction systems, the **Mn_3Mn** complex being easier to reduce than the **Mn_3Ca** and **{Mn_3Sr}$_2$** complexes (Table S15). This result highlights that the pyridine-carboxylate motifs, when coordinated to a metal, can be reversibly reduced, similarly to the well-known redox behavior of bipyridine ligands.

The **Mn^{III}_3M** species are quantitatively generated by exhaustive electrolyses carried out at a potential of 1.20 V after the exchange of about 2.6-2.9 electrons confirming that each oxidation wave corresponds to the exchange of one-electron. After electrolysis, for the three complexes, all the reversible waves are maintained located either in the positive and negative

potential regions with the same intensity and at the same potential, again confirming the excellent stability of the MC structures including the preservation of the cations in the central cavity, even in the three-electrons oxidized state (Figures 6 and S3). It is important to note that given the particular geometry of the tpada^{2-} ligand, the Mn^{2+} as well as the Mn^{3+} ions in the {Mn(tpada)} units forming the macrocycle in the initial **Mn^{II}_3M** and oxidized forms **Mn^{III}_3M** are hepta-coordinated, an unusual coordination number especially for a Mn^{3+} ion.[35, 55]

Solutions of the initial and oxidized compounds were studied by UV-visible absorption and EPR spectroscopies (Figures 7 and S4-S5). The yellow pale solutions of the initial **Mn^{II}_3M** complexes absorb only in the UV region (shoulders around 350 nm) in accordance with high-spin Mn^{II} species.[55] On the other hand, orange solutions of the **Mn^{III}_3M** complexes generated by exhaustive electrolyses at 1.2 V exhibit absorption bands in the visible (Figures 7 and S4) in agreement with the generation of Mn(III) species: a narrow band at 450 nm associated with a shoulder at 500 nm and a broad band of lower intensity centered at around 720 nm.[56] The relative intensity of these bands, as well as the value of the λ_{max}, slightly vary with the nature of the complexes. This variation, although minimal, confirms the electrochemical results, *i. e.* the central ions remain also coordinated in the oxidation state **Mn^{III}_3M**.

The X-band EPR spectra of the complexes before and after electrolysis at 1.2 V have been recorded at 100 K (Figure S5). In the initial state, the spectra are all comparable and present a main transition centered around g = 2 (340 mT) characteristic of a high spin manganese(II) signal (S = 5/2). Although the spectra are similar, the transition width is variable, suggesting small variations of the D parameter,[57-58] and thus that the central cation has a weak influence on the electron properties of the Mn^{2+} ions of the metallamacrocycle. For the **Mn^{III}_3Ca** and **Mn^{III}_3Sr** complexes, after exhaustive electrolysis at 1.2 V, no transition is visible on the EPR spectra demonstrating the effective oxidation of the three Mn^{2+} of the metallamacrocycle into Mn^{3+}. Indeed, the manganese(III), a d^4 ion with integer spin, is EPR silent at 100 K at X-band frequencies. By contrast, the EPR spectrum of the mixed valence **$Mn^{III}_3Mn^{II}$** species reveals a 6-line EPR signal. This signal, only detected for the **Mn^{III}_3Mn** complex, corresponds to the central Mn(II) since the three Mn(II) ions of the macrocycle are oxidized to Mn(III). In addition, the presence of a 6-line signal and not a multiplet for this complex indicates that the central Mn(II) is fully isolated and does no communicate with its Mn(III) neighbors forming the macrocycle.

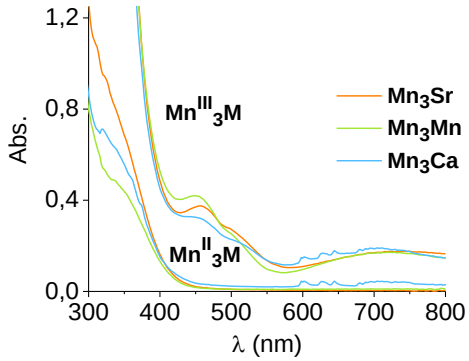

Figure 7: UV-Visible absorption spectra of solutions of **Mn$_3$Mn** (0.64 mM) (green), **Mn$_3$Ca** (0.57 mM) (blue) and **{Mn$_3$Sr}$_2$** (0.33 mM) (red) in CH_3CN, 0.1 M $[Bu_4N]ClO_4$ before and after exhaustive electrolysis at +1.2 V (generation of **Mn$^{III}_3$Mn^{II}**, **Mn$^{III}_3$Ca** and **Mn$^{III}_3$Sr**). Optical path of 1 cm.

This electrochemical study revealed interesting properties for these tetranuclear **Mn$^{II}_3$M** complexes featuring a MC structure, namely an excellent stability both in their initial state and in their three-electron oxidized state, **Mn$^{III}_3$M**. We have thus compare this behavior with those of similar manganese(II) complexes already described in the literature. First, it appears that the redox behavior observed is quite unusual for manganese(II) multinuclear species with μ-carboxylato bridges and similar pyridine-based multidentate ancillary ligands. For example, the cyclic voltammograms of bis-μ-acetato binuclear complexes of the type $[Mn^{II}_2(\mu_{1,3}\text{-}O_2CCH_3)_3(bpea)_2]^+$ and $[Mn^{II}_2(\mu_{1,3}\text{-}O_2CCH_3)_2(tpa)_2]^{2+}$ (bpea = N,N-bis-(2-pyridylmethyl)ethylamine) and tpa = tris(2-methylpyridyl)amine) exhibit in acetonitrile fully irreversibly oxidation processes, their oxidation leading to the quantitative formation of the μ-oxo $[Mn^{III}_2(\mu\text{-}O)(\mu_{1,3}\text{-}O_2CCH_3)_2(bpea)_2]^{2+}$ and $[Mn^{III}_2(\mu\text{-}O)(\mu_{1,3}\text{-}O_2CCH_3)(tpa)_2]^{3+}$, respectively. Upon oxidation into the +III oxidation state of manganese, a fast decoordination of an acetato bridge of the complexes with the concomitant formation of an oxo bridge by coordination and deprotonation of a residual water molecule of the solvent occurs.[56, 59-60] The tendency of Mn(III) ions to form μ-oxo bridges[60] has also been demonstrated for other binuclear manganese(II) complexes with μ-carboxylato bridges of the type $[Mn^{II}_2(L)_2(H_2O)_2$ (L = N-glycyl-N'-methyl/benzyl-N,N'-bis(2-pyridylmethyl)-1,2-ethanediamine) for which the carboxylate bridges are provided by the pentadentate L ligands[61]. The latter also exhibit irreversible oxidation processes in acetonitrile. By contrast, the stability of the **Mn$^{III}_3$M** MC structure can be explained by the presence of the M^{2+} cation very strongly bound to the macrocycle *via* six μ-carboxylato bridges from three $tpada^{2-}$ ligands. In addition, the fact that

these carboxylates are provided by the ancillary ligands certainly contributes to the excellent stability of the whole structure even in its oxidized form, by preventing their decoordination and the subsequent formation of μ-oxo bridged species in the +III oxidation state of manganese.

These 12-MC-3 **Mn_3M** complexes are analogues of the iron complexes $[Fe^{II}_3Fe^{II}(bpg)(O_2CPh)_3]^{2+}$ and $[Fe^{II}_3Fe^{II}(bpg)(O_2CCH_3)_3]^{2+}$ synthesized by Que and coworkers with the tetradentate monocarboxylate bpg^- ligand (Figure 2A(c)).[38-39] Nevertheless, since two carboxylates are already incorporated in the ancillary $tpada^{2-}$ ligand, the synthesis of **Mn_3M** do not require additional carboxylates to coordinate the central metal M. Indeed only one of the two carboxylate units of each $tpada^{2-}$ ligand is engaged in the macrocycle, the second one being available for the coordination of the cation located in the central cavity. Since, the electrochemical properties of these iron complexes were not investigated, neither those of the other carboxylate bridged metallamacrocycle complexes, it is therefore not possible to compare their stability in their initial and oxidized forms with those of the **Mn_3M** complexes.

The inherent structural stability in CH_3CN solution was also established by mass spectrometry and electrochemistry for the family of structurally related heterometallic pentanuclear Mn^{III}_4Ca complexes, $[Mn^{III}_4Ca(O_2CR)_4(shi)_4]^{2-}$ (Figure 2B(b-c)).[42, 45-46] In these complexes featuring a distorted square pyramidal topology with the four Mn(III) atoms forming the square base, the central Ca^{2+} in the apical position is maintained through four additional carboxylates (O_2CR). Due to the pronounced stability of the $Mn_4{}^{III}Ca$ MC core induced by the four donor atoms of the salicylhydroximate ligand, these compounds are also very rare examples of metal clusters that retain their solid-state structures in solution (CH_3CN solvent). The cyclic voltammetry of these complexes exhibits only one reversible oxidation system, attributed by the authors to a mono-electronic oxidation, and poorly defined reduction peaks. This electrochemical behavior is however very different to that of the **Mn^{II}_3M** complexes, which underlines the unusual properties of the latter. In addition, the stability of the reduced complex Mn^{II}_4Ca was not evaluated by bulk electrolysis.

Finally, the heterometallic **Mn_3Ca** and **$\{Mn_3Sr]_2$** also join a growing, but still small, family of heteronuclear manganese-calcium complexes and even rarer manganese-strontium complexes as models of the native OEC of photosystem II. Table 1 gives an overview of all the synthetic **Mn-Ca** and **Mn-Sr** heterometallic compounds structurally characterized to date. The compounds are classified on the basis of their structures, polymeric compounds or

discrete molecules, and on the chemical nature of the bridge(s) between the Mn and Ca/Sr cations, μ-carboxylato, μ-hydroxo, μ-alkoxo, μ-oxo, or a combination of different bridges. If the large majority of these complexes present a structure quite different from that of the OEC, some very close structural models of the native OER and Sr-substituted OEC were obtained by the groups of Agapie and co-workers,[32-33, 50] Christou and co-workers[30] and Zhang and co-workers,[28, 31] with the $\{Mn_3CaO_4\}$, $\{Mn_4CaO_4\}$, $\{Mn_3Ca_2O_4\}$ or $\{Mn_3CaAgO_4\}$ stoichiometry. These complexes containing the $\{Mn_3CaO_4\}$ or $\{Mn_3SrO_4\}$ cubane core and in some case a dangling metal cation (Mn, Ca or Ag) mimicking the fourth external Mn attached through one μ_4-oxo of the cubane. Although the structure of the **Mn_3Ca** and **$\{Mn_3Sr]_2$** compounds are not similar to that of the OEC, the X-ray structures corroborate the high tendency of calcium and strontium to coordinate water molecule as found in the native and Sr-substituted OEC. In addition, such self-assembled Mn^{2+}-Ca complexes bridged by carboxylate units could be relevant for mimicking the first stages of the OEC assembly process.

Table 1. Chemical Formulas of the Structurally Characterized Heterometallic Mn-Ca and Mn-Sr Complexes with Various Ancillary Ligands[a] Reported to Date Classified on the basis of the Chemical Nature of the Link Between Mn and Ca/Sr Cations and their Main Structural Features Relevant to the Native OEC.

Complex	Structural features relevant to the OEC	Author year[ref]
μ-carboxylato bridged Mn(II/III)-Ca(II) polymers		
$[Mn^{II}Ca(mal)_2(H_2O)_4]_n$	2 water molecules coordinated to Ca and Mn^{II}	Rojo 2000[62]
$[Mn^{II}Ca_2(bipy)_2(DCA)_6(H_2O)(MeOH)]_n$	2 water molecules coordinated to Mn^{II}	Benniston, Bartolomé 2014 [63]
$[Mn^{III}{}_3CaNa(sal)_6(H_2O)_6]_n$	water molecules coordinated to Ca and Mn^{III} (from 1 to 3)	Chen 2010[64]
$\{[Mn^{III}{}_6Ca_2O_2(Me\text{-}saO)_6(prop)_6(H_2O)_2]\}_n$	$[Mn^{III}{}_3CaO(OR)_3(NO)_2]^{3+}$ tetrahedron as in the Mn_3CaO_4 distorted-cubane subunit of the OEC	Milios 2011 [65]
μ-carboxylato-bridged Mn(II)-Ca(II)/Sr(II) clusters		
$[Mn^{II}{}_2Ca_2(tpaa)_2(OH_2)_{12}][Mn^{II}(tpaa)]_2$ $[Mn^{II}Ca(tpada)Cl(OH_2)_3(MeOH)_2]^-$	water molecules coordinated to Ca (from 1 to 7) involved in intra and intermolecular H-bond networks	Collomb 2015[34-35]
$[Mn^{II}{}_3Ca(tpada)_3(OH_2)]^{2+}$ $[Mn^{II}{}_3Sr(tpada)_3(OH_2)]_2{}^{4+}$	water molecules coordinated to Ca and Sr (from 1 to 2)	Collomb [This work]
μ-hydroxo-bridged Mn(III)-Ca(II)/Sr(II) binuclear complexes		
$[Mn^{III}Ca(OH)(15\text{-}crown\text{-}5)(MST)]^+$	$Ca^{II}(\mu\text{-}OH)Mn^{III}$ motif proposed to be present in the OEC S_1 state	Borovik 2011[66-67]
$[Mn^{III}Sr(OH)(15\text{-}crown\text{-}5)(MST)]^+$		Borovik 2013[68]
μ-alkoxo-bridged Mn(II/III)-Ca(II) cluster		
$[Mn^{II}{}_4Ca_2Cl_4(\mu\text{-}OEtOMe)_8]$	-	Sobota 2007[69]
$[Mn_2{}^{II}Ca_2(L^S)_2(DMF)_2]$ $[Mn^{II}Ca_2(HL^S)_2(DMF)_2]$	-	Koutsantonis 2015[70]
$[Mn^{III}{}_2Ca_2(hmp)_6(H_2O)_4(MeCN)_2]^{4+}$	2 water molecules coordinated to Ca	Arauzo 2017[22]
$[Mn^{III}{}_2Ca_2(hmp)_6(NO_3)_2(ClO_4)_2(H_2O)_2]$ $[Mn^{III}{}_2Ca_2(hmp)_6(CBA)_2(H_2O)_4]^{2+}$ $[Mn^{III}{}_2Ca_2(hmp)_6(DCA)_2(NO_3)_2(H_2O)_2]$	$CaMn_2O_3$ cuboid structures arrangements - water molecules coordinated to Ca (from 1 to 2)	Shova, Benniston 2017[21]
μ-carboxylato and μ-alkoxo-bridged Mn(III/IV)-Ca(II) clusters		

$[Mn^{III}_4Ca(O_2CPh)_4(shi)_4]^{2-}$	1rst family of oxo-free complexes with same Mn/Ca stoichiometry as the OEC but with a different arrangement	Christou, Stamatatos 2011[45]
$[Mn^{III}_4Ca(L^1)_4(shi)_4]^{2-}$ $[Mn^{III}_4Ca(L^2)_4(shi)_4]^{2-}$ $[Mn^{III}_4Ca(L^2)_4(shi)_4(shiH_2)_2]^{4-}$ $[Mn^{III}_4Ca(L^3)_4(shi)_4]^{2-}$	same Mn/Ca ratio as the OEC but with a different arrangement	Christou, Stamatatos 2015[46]
$[Mn^{III}_4Ca_2(O_2CPh)_4(shi)_4(H_2O)_2((Me)_2CO)]$	1 water molecule coordinated to Ca	Stamatatos 2017[26]
$[Mn^{II}_2Mn^{III}_4Ca_2Cl_2(O_2CPh)_7(shi)_4(py)_4]^-$	-	
$[Mn^{III}_4Mn^{IV}_4Ca(OEt)_2(shi)_{10}(EtOH)_2]^{2-}$ $[Mn^{III}_8Ca_2(CO_3)(shi)_8]^{4-}$	-	
μ-alkoxo and μ-oxo-bridged Mn(III/IV)-Ca(II) clusters		
$[Mn^{III}_3Mn^{II}CaO(L^4)_3Cl_2(O_2CMe)_{1.2}(H_2O)_{1.5}(MeOH)_{0.3}]^+$	1rst isolated oxo-bridged complex with same Mn/Ca stoichiometry as the OEC but with a different arrangement - possible model of the OEC $Mn^{III}_3Mn^{II}$ S_0 state	Powell 2006[71]
$[Mn^{III}_3CaNaO(L^5\text{-}H)_3(N_3)_3(MeOH)]^+$	-	Powell and Reedjik 2011[72]
μ-carboxylato- and μ-oxo-bridged Mn(III/IV)-Ca(II)/Sr(II) clusters		
$[Mn^{II}_2Mn^{III}_{10}Mn^{IV}Ca_2O_{10}(OH)_2(OMe)_2(O_2CPh)_{18}(H_2O)_4]$	2 types of Mn_4CaO_4 pseudo-cubane moities with one similar to the OEC	Christou 2005[73]
$[Mn^{II}Mn^{III}_{13}SrO_{11}(OMe)_3(O_2CPh)_{18}(MeCN)_2]$	1rst Mn-Sr cluster isolated	Christou 2007[74]
$[Mn^{IV}_3Ca_2O_4(O_2C^tBu)_8(^tBuCO_2H)_4]$	1rst model of the asymmetric Mn_4CaO_4 OEC cluster: a $[Mn^{IV}Ca_2O_4]$ carboxylate cubane core but with an external Ca attached to one oxo of the cubane - EPR spectra similar to OER S_2 state	Christou 2012[30]
$[Mn^{III}_2Mn^{IV}_2CaO_4(O_2C^tBu)_8(^tBuCO_2H)_2(py)]$	1rst closest mimic of the asymmetric Mn_4CaO_4 OEC cluster, model of the OER S_1 state	Zhang, Dong, Dau 2015[31]
$[Mn^{III}_2Mn^{IV}_2CaO_4(O_2C^tBu)_8(^tBuCO_2H)(py)(MeCN)]$ $[Mn^{III}_2Mn^{IV}_2CaO_4(O_2C^tBu)_8(py)(DMF)_2]$	closest mimic of the asymmetric Mn_4CaO_4 OEC cluster including exchangeable solvent molecules (MeCN or DMF)	Zhang 2019[28]
$[Mn^{IV}_6Ca_2O_9(O_2C^tBu)_{10}(H_2O)_4]$ $[Mn^{IV}_6Ca_2O_9(O_2C^tBu)_{10}(H_2O)_3(CH_3CO_2C_2H_5)]_5$ $[Mn^{IV}_6Ca_2O_9(O_2C^tBu)_{11}]$	3 distorted $Mn_2Ca_2O_4$ cubane moities sharing a trigonal-bipyramidal Ca_2O_3 unit in the center	Zhang, Dong 2015[75]
$[Mn^{IV}_6Sr_4O_9(O_2C^tBu)_{10}(^tBuCO_2H)_2(py)_2]$	1rst isolated cluster displaying all of the three types of μ-oxo moieties observed in the OEC (μ_2-O^{2-}, μ_3-O^{2-} and μ_4-O^{2-})	Zhang, Dong 2014[76]
$[Mn^{IV}_6Ca_2O_9(O_2CPh^tBu)_{10}(^tBuPhCO_2H)_5]$ $[Mn^{IV}_6Sr_2O_9(O_2CPh^tBu)_{10}(^tBuPhCO_2H)_5]$	3 fused $Mn_2Ca_2O_4$ cubanoids sharing a trigonal-bipyramidal Ca_2O_3 unit in the center	Corbella 2015[77]
$[Mn^{IV}_6Ca_2O_9(OMe)_2(O_2C^tBu)_{14}(^tBuCO_2H)_4(H_2O)_{0.3}]$	*2* $Mn_3Ca_2O_4$ cubic unit similar to the OEC cubane subunit	Bikas, Najafpour 2020[23]
μ-carboxylato-, μ-alkoxo and μ-oxo-bridged Mn(II/III/IV)-Ca(II) clusters		
$\{[Mn^{II}Mn^{III}_2O(O_2CMe)_3L^6]_2Ca\}^{2+}$	-	Agapie 2011[32]
$[Mn^{IV}_3CaO_4(O_2CMe)_3L^6(THF)]$	1rst accurate model of the cubane subsite Mn_3CaO_4 of the OEC	
$[Mn^{IV}Mn^{III}_2CaO_2(O_2CMe)_2L^6(DME)(OTf)]^{2+}$ $[Mn^{IV}Mn^{III}_2CaO_2(O_2CMe)_2L^6(H_2O)_3]^{3+}$ $[Mn^{III}_3CaO_2(O_2CMe)_2L^6(DME)(OTf)]^+$ $[Mn^{IV}Mn^{III}_2SrO_2(O_2CMe)_2L^6(DME)(OTf)]^{2+}$ $[Mn^{III}_3SrO_2(O_2CMe)_2\ L^6(DME)(OTf)]^+$	-	Agapie 2013[54]
$\{[Mn^{IV}_3SrO_4(O_2CMe)_3L^6(DMF)]\}_2$	Mn_3SrO_4 cubane clusters structurally related to the Sr-substituted $Mn^{IV}_3SrO_4$ OEC cluster	Agapie 2013[50]
$[Mn^{IV}_3CaO_3(OH)(O_2CMe)L^6(ON_4O)]^+$	asymmetric cubanoid with one protonated oxo bridge	Agapie 2014[33]
$[Mn^{IV}_3CaAgO_4(O_2CMe)L^6(ON_4O)(OTf)]$	models the topology of the OEC: a cubane motif with a dangling transition metal	
$[Mn^{II}_2Mn^{III}_2CaO_2(O_2CR)_5L^{6'}(THF)]$	rare example of cluster of same metal stoichiometry with oxo bridges, as the OEC	Agapie 2017[20]

$[Mn^{III}_6Ca_2O_3(hmp)_6(BA)_6(H_2O)_6]^{4+}$	Ca coordinated by 3 water molecules involves in H-bonding network	Shova, Benniston 2017[21]
$[Mn^{II}_6Mn^{III}_{16}Ca_2O_{14}(OH)_4(OMe)_6(O_2CPh)_{22}(qao)_2(MeCN)_2(H_2O)_4]^{2+}$	highest in nuclearity Mn-Ca cluster includes several $\{Mn_4CaO_x\}$cubane subunits	Stamatatos 2018[27]
$[Mn^{IV}_2Ca_2(OMe)_2(NO_3)_2(dapdo)_4]$	-	
$[Mn^{III}_3CaO(OH)(mAla)(O_2CPh)_3(HL^7)_2(MeOH)]_2$	Mn_3Ca tetrahedron similar to the OEC the sp^2 N-atom of the mAla Schiff base ligand mimicks the amide N-atoms present in the OEC	Milios 2020[29]

[a] mal = malonate; bipy = 2,2'-bipyridine; H-DCA = dichloroacetic acid; sal = salicylate; prop = propionate; Me-saOH$_2$ = 2-hydroxyphenylethanone oxime; H_3-tpaa = 6,6',6''-nitrilotris(methylene)tripicolinic acid); H_2-tpada = 6,6'-(pyridin-2-ylmethylazanediyl)bis(methylene)dipicolinic acid ; $[MST]^{3-}$ = N,N',N''-[2,2',2''-nitrilotris(ethane-2,1-diyl)]tris(2,4,6-trimethylbenzenesulfonamido); MeOEtOH = 2-methoxyethanol; H_4-L^S = *p*-*t*-butylthiacalixarene; DMF = dimethylformamide;
hmp-H = 2-(hydroxymethyl)pyridine; H-CBA = 3-chlorobenzoic acid; shi-H_3 = salicylhydroxamic acid; L^1-H = 2-naphthoic acid ; L^2-H = 9-anthracenecarboxylic acid; L^3-H = 1-pyrenecarboxylic acid; L^4-H_2 = 2-[[(2-hydroxypropyl)imino]methyl]-6-methoxyphenyl; L^5-H_3 = 2-(2,3-dihydroxypropyliminomethyl)-6-methoxyphenol; py = pyridine; ^{t}BuPhCO$_2$H = *p*-*tert*-buthylbenzoic acid; L^6-H_3 = 1,3,5-tris(2-di(2'-pyridyl)hydroxymethylphenyl)benzene; THF = tetrahydrofuran; DME = 1,2-dimethoxyethane; $L^{6'}$-H_3 = 2-{2,4-bis(2-di(2'-pyridyl)hydroxymethylphenyl)phenyl}benzoic acid; H-BA = benzoic acid; qao-H = quinoline-2-aldoxime; dapdo-H_2 = 2,6-diacetylpyridine dioxime; mAla-H = methylalanine; H_3-L^7 = 2-(β-naphthalideneamino)-2-hydroxyethyl-1-propanol.

Conclusion

A series of new manganese(II) homo- and heterometallic tetranuclear complexes having a 12-metallacrown-3 type arrangement, including a central cation within their cavity (Mn^{2+}, Ca^{2+} or Sr^{2+}), have been spontaneously self-assembled at room temperature by reacting Mn^{2+} with the hexadentate tripodal $tpada^{2-}$ ligand incorporating two carboxylate functions. These complexes constitute rare examples of metallacrowns incorporating μ-carboxylate bridges between the various metals. The heterometallic **Mn_3Ca** and **$\{Mn_3Sr]_2$** also join the small family of heteronuclear manganese-calcium complexes and even rarer manganese-strontium complexes as models of the OEC of photosystem II. Solution studies carried out in organic solvent (CH_3CN), either by mass spectrometry and electrochemistry coupled to UV-visible and EPR spectroscopy confirmed their structural integrity in solution. It appears that these complexes present a very rich redox behavior with up to eight reversible waves detected by cyclic voltammetry, three corresponding to the successive oxidation of the Mn(II) ion constituting the macrocycle into Mn(III) and five to the reduction of the $tpada^{2-}$ ligand. The **Mn^{III}_3M** three-electrons oxidized species have been quantitatively generated by bulk electrolyses at 1.20 V demonstrating the high stability of the tetranuclear structure also in the three-electrons oxidized state. This redox behavior, quite unusual for Mn(II) compounds coordinated with such ligands, can be correlated to the presence of the central M^{2+} cation

within the cavity strongly linked to the three Mn(II)/Mn(III) ions constituting the ring through six bridging carboxylate ligands of the three $tpada^{2-}$ ligands, that stabilizes the structure.

These 12-MC-3 complexes are analogues of iron complexes synthesized by Que with the tetradentate monocarboxylate ligand Hbpg (Figure 2A(c)), but unlike these complexes, their synthesis does not require the addition of supplementary carboxylates to coordinate the central metal since these are already an integral part of the ancillary ligand. Indeed, only one of the two carboxylate units of each $tpada^{2-}$ ligand is involved in the macrocycle, the second unit being free to coordinate the central cation. The presence of this second carboxylate within the ligand framework is most probably also at the origin of the excellent stability of these structures in solution, even in their three-electron oxidized form. Anyway, the electrochemical properties of these complexes cannot be compared with those of the few examples of previously published μ-carboxylato bridged MCs, since the electrochemical properties of this family of complexes have never been studied.

Finally, it should be highlighted that due to the particular geometry of the $tpada^{2-}$ ligand, the Mn^{2+} but also the Mn^{3+} ions in the $\mathbf{Mn^{II}_3M}$ and $\mathbf{Mn^{III}_3M}$ complexes are hepta-coordinated, an unusual coordination number especially for a Mn(III) ion. In addition, the calcium and strontium in the isolated structures incorporate water molecule, as found in the OEC of PSII.

In future works, it will be interesting to explore other experimental conditions in view to test the possibility to access such MC complexes with the $tpada^{2-}$ ligand without any cation within the central cavity, to determine the affinity of this structure for the coordination of different cations in the context of ionic recognition. We will also explore the synthesis of new complexes with other metal cations by using this tripodal hexadentate $tpada^{2-}$ ligand that gives rise to original and stable structures, unusual coordination number for metal cations and electrochemical properties with reversibility of the oxidation and reduction processes.

Experimental section

Materials. All solvents and reagents were laboratory reagent grade or better and used as received. Potassium hydroxide (KOH, Sigma-Aldrich, ≥ 85%), tetra-*n*-butylammonium hydroxide $[Bu_4N]OH$ (1.0 M in methanol, Alfa Aesar), manganese(II) acetate tetrahydrate ($Mn(O_2CCH_3)_2{\cdot}4H_2O$, Merck), lithium perchlorate anhydrous ($LiClO_4$, ≥ 98%, Sigma-Aldrich), calcium trifluoromethanesulfonate anhydrous ($Ca(CF_3SO_3)_2$, Aldrich, 99.9%), strontium nitrate anhydrous ($Sr(NO_3)_2$, 99+%, Strem) were used as received. Acetonitrile

(CH_3CN, Fisher, HPLC grade), and tetra-n-butyl-ammonium perchlorate ($[Bu_4N]ClO_4$, Fluka) for electrochemical measurements were stored under an argon atmosphere in a dry-glove box.

Synthesis of 6,6'-(pyridin-2-ylmethylazanediyl)bis(methylene)dipicolinic acid (H_2tpada). This ligand was synthetized as previously described.{Gerey, 2015 #3350} The fraction isolated corresponds to the triprotonated form, H_3tpada(PF_6). Anal. Calcd. for $C_{20}H_{19}N_4O_4PF_6 \cdot H_2O$ (542.37): C, 44.29; H, 3.9; N, 10.33. Found: C, 44.23; H, 3.79; N, 10.00.

Synthesis of the complexes

Caution! *Perchlorate salts of compounds containing organic ligands are potentially explosive. Although we have encountered no such problems, only small quantities of these compounds should be prepared and handled with care.*

Synthesis of $[\{Mn^{II}(tpada)\}_3Mn^{II}](X)_2$ ($Mn_3Mn(X)_2$) (X = ClO_4 or PF_6). 3.0 equiv. of KOH (0.1 M, 19.2 mg, 0.342 mmol) was added to a stirred solution of the ligand (H_3tpada)$PF_6 \cdot H_2O$ (62 mg, 0.114 mmol) in 8 mL of methanol, To this colorless solution, 2 mL of a methanol solution containing 1.4 equiv of $Mn^{II}(O_2CCH_3)_2 \cdot 4H_2O$ (39.3 mg, 0.16 mmol) was added under vigorous stirring. The resulting slightly yellow solution was stirred 30 min and then partially evaporated under reduced pressure until 2 mL leading to the formation of a yellow microcrystalline powder corresponding to $[\{Mn(tpada)\}_3Mn](PF_6)_2 \cdot 3H_2O$, which was filtered, washed with diisopropyl ether and dried under vacuum. Single crystals suitable for X-ray diffraction were only obtained as perchlorate salts. The yellow powder of $[\{Mn(tpada)\}_3Mn](PF_6)_2 \cdot 3H_2O$ was redissolved in acetonitrile and an excess of $LiClO_4$ was added. Slow diffusion of diethyl ether or ethyl acetate into the solution leads to the formation of single crystals of $[\{Mn(tpada)\}_3Mn](ClO_4)_2 \cdot 2CH_3CN$ (yield, 60 mg, 97%). Anal. Calcd. for $C_{60}H_{48}N_{12}O_{12}Mn_4P_2F_{12} \cdot 3H_2O$ (1692.82): C, 42.57; H, 3.22; N, 9.93. Found: C, 42.44; H, 3.19; N, 9.87. ESI-MS *m/z* for $C_{60}H_{48}N_{12}O_{12}Mn_4P_2F_{12}$ (M): 674.1 $[M\text{-}2PF_6]^{2+}$, 1493.1 $[M\text{-}PF_6]^+$. IR (KBr pellet, cm^{-1}): 3416 (m), 1623 ($\mu_{asCOO\text{-}}$, s), 1594($\mu_{asCOO\text{-}}$, vs), 1466 (sh), 1440 ($\mu_{sCOO\text{-}}$, m), 1386 ($\mu_{sCOO\text{-}}$, s), 1277 (m), 1183 (w), 1156 (w), 1121 (w), 1102 (w), 1078 (m), 1055 (w), 1019 (m), 980 (w), 955 (w), 845 (PF_6, vs), 773 (s), 690 (m), 639 (w), 558 (PF_6, s), 512 (w), 457 (w).

Synthesis of $[\{Mn^{II}(tpada)\}_3Ca(OH_2)](PF_6)_2$ ($Mn_3Ca(PF_6)_2$). 3.0 equiv. of $^nBu_4NOH$ (1.0 M, 342 µL, 0.342 mmol) was added to a stirred solution of (H_3tpada)$PF_6 \cdot H_2O$ (62 mg, 0.114 mmol) in 8 mL of methanol, 28.0 mg (1.0 equiv., 0.11 mmol) of $Mn(O_2CCH_3)_2 \cdot 4H_2O$ was

dissolved in 2 mL of MeOH and added to the colorless solution of deprotonated ligand under vigorous stirring. Then, a solution $Ca(CF_3SO_3)_2$ in 2 mL acetonitrile (38.7 mg, 0.11 mmol) was quickly added to the solution. The resulting slightly yellow solution was stirred 30 min and then partially evaporated under reduced pressure until 2 mL leading to the precipitation of a yellow crystalline powder. X-ray diffraction suitable crystals of $[\{Mn^{II}(tpada)\}_3Ca(OH_2)](PF_6)_2 \cdot 0.25CH_3CN \cdot 1.75CH_3CO_2C_2H_5$ were obtained by slow diffusion of diethylether or ethyl acetate into an acetonitrile solution of this compound (yield, 60 mg, 88%). Anal. Calcd. for $C_{60}H_{50}N_{12}O_{13}Mn_3CaP_2F_{12}$ (1641,93): C, 43.89; H, 3.07; N, 10.24. Found: C, 43.70; H, 3.13; N, 10.21. ESI-MS *m/z* for $C_{60}H_{50}N_{12}O_{13}Mn_3CaP_2F_{12}$ (M): 666.6 $[M\text{-}H_2O\text{-}2PF_6]^{2+}$, 1478.1 $[M\text{-}H_2O\text{-}PF_6]^{+}$. IR (KBr pellet, cm^{-1}): 3436 (m), 1625 (μ_{asCOO-}, s), 1594 (μ_{asCOO-}, vs), 1467 (sh), 1440 (μ_{sCOO-}, m), 1388 (μ_{sCOO-}, s), 1277 (m), 1185 (w), 1157 (w), 1122 (w), 1102 (w), 1078 (m), 1055 (w), 1032 (sh), 1018 (m), 981 (w), 955 (w), 847 (PF_6, vs), 774 (s), 690 (m), 640 (w), 558 (PF_6, s), 524 (w), 453 (w).

Synthesis of $[\{Mn^{II}(tpada)\}_3Sr^{II}(OH_2)]_2(PF_6)_4$ ($\{Mn_3Sr\}_2(PF_6)_2$). 3.0 equiv. of $^nBu_4NOH$ (1.0 M, 342 µL, 0.342 mmol) was added to a stirred solution of $(H_3tpada)PF_6 \cdot H_2O$ (62 mg, 0.114 mmol) in 8 mL of methanol. 28.0 mg (1.0 eq., 0.11 mmol) of $Mn(O_2CCH_3)_2 \cdot 4H_2O$ was dissolved in 2 mL of MeOH and added to the mixture under vigorous stirring. Then, a CH_3CN/H_2O (2 mL/0.5 mL) solution of $Sr(NO_3)_2$ (25 mg, 0.12 mmol) was quickly added to the solution. The resulting slightly yellow solution was stirred 30 min and then partially evaporated under reduced pressure until 2 mL leading to the precipitation of a yellow crystalline powder. Single crystals suitable for X-ray diffraction of $[\{Mn^{II}(tpada)\}_3Sr^{II}(OH_2)]_2(PF_6)_4 \cdot 2CH_3OH \cdot 1.5CH_3CO_2C_2H_5 \cdot 0.5H_2O$ were obtained by slow diffusion of ethyl acetate in acetonitrile (yield, 62 mg, 91%). Anal. Calcd. for $C_{120}H_{100}N_{24}O_{26}Mn_6Sr_2P_4F_{24} \cdot 4CH_3CN \cdot 2H_2O$ (3461.05): C, 42.95; H, 3.27; N, 10.96. Found: C, 42.94; H, 3.93; N, 11.49. ESI-MS *m/z* for $C_{60}H_{50}N_{12}O_{13}Mn_3SrP_2F_{12}$ ($[\{Mn^{II}(tpada)\}_3Sr^{II}(OH_2)](PF_6)_2$ (M)): 690.7 $[M\text{-}H_2O\text{-}2PF_6]^{2+}$, 1526.0 $[M\text{-}H_2O\text{-}PF_6]^{+}$. IR (KBr pellet, cm^{-1}): 3436 (m), 1731 (w), 1626 (μ_{asCOO-}, s), 1591 (μ_{asCOO-}, vs), 1439 (μ_{sCOO-}, m), 1385 (μ_{sCOO-}, s), 1276 (w), 1188 (w), 1154 (w), 1122 (w), 1077 (w), 1017 (w), 849 (PF_6, vs), 773 (vs), 688 (m), 558 (PF_6, s), 445 (w).

Synthesis of $[Sr(tpada)(OH_2)]_4$ (Sr_4). A suspension of $Sr(OH)_2 \cdot 8H_2O$ (39.5 mg, 148.6 µmol) in water (0.5 mL) was added dropwise to a suspension of $(H_3tpada)PF_6 \cdot H_2O$ (38.5 mg, 71 µmol) in water (3.5 mL), yielding to the solubilisation of the ligand. Precipitation of a white

solid slowly occurred over 30 minutes under stirring. The solid was then filtered off and dried under vacuum. It was redissolved in a DMF:MeCN mixture (50:50, 7 mL), solid impurities were filtered off, and single crystals of $[Sr(tpada)(OH_2)]_4 \cdot 8CH_3CN \cdot 2H_2O$ (yield, 6 mg, 16 %) were obtained by slow diffusion of diisopropyl ether into the solution. Anal. Calcd. for $C_{80}H_{72}N_{16}O_{20}Sr_4 \cdot 1.1DMF \cdot 3.5H_2O$ (2071.46): C, 48.3; H, 4.22; N, 11.56. Found: C, 48.35; H, 4.37; N, 11.37.

ASSOCIATED CONTENT

Supporting Information.

This Supporting Information is available free of charge on the ACS Publications website.

Materials and general experimental details. Additional data for X-ray structure determination, mass spectrometry, electrochemistry, UV-visible absorption and EPR spectroscopy (Tables S1-S15, Figures S1-S5).

Accession Codes

CCDC 2059900, 2059901, 2059902 and 2059903 contain the supplementary crystallographic data for this paper. These data can be obtained free of charge via www.ccdc.cam.ac.uk/data_request/cif or by emailing data_request@ccdc.cam.ac.uk, or by contacting The Cambridge Crystallographic Data Centre, 12 Union Road, Cambridge CB2 1EZ, U.K.; fax: +44 1223 336033

AUTHOR INFORMATION

Corresponding Authors

*E-mail: marie-noelle.collomb@univ-grenoble-alpes.fr

ORCID

Florian Molton: 0000-0001-6675-5551

Jérôme Fortage: 0000-0003-2673-0610

Marie-Noëlle Collomb: 0000-0002-6641-771X

Author Contributions

The manuscript was written through contributions of all authors. All authors have given approval to the final version of the manuscript.

Notes

The authors declare no competing financial interest

ACKNOWLEDGEMENTS

This work has been partially supported by the French National Research Agency through Labex ARCANE and CBH-EUR-GS (ANR-17-EURE-0003) for the project MnCaPSII, as well as ANR-13-BS07-0015-01 (MnCaOEC) including the E.G. postdoctoral grant. B.G. thanks the "Université Grenoble Alpes" for his PhD grant. We thank the IR-RPE CNRS FR3443 RENARD network for EPR facilities. The NanoBio-ICMG platforms (FR 2607) are acknowledged for their support. This work was also supported by COST CM1202 program (PERSPECT H_2O).

References

1. Gerey, B.; Gouré, E.; Fortage, J.; Pécaut, J.; Collomb, M.-N., Manganese-calcium/strontium heterometallic compounds and their relevance for the oxygen-evolving center of photosystem II. *Coord. Chem. Rev.* **2016,** *319*, 1-24.
2. Najafpour, M. M.; Zaharieva, I.; Zand, Z.; Maedeh Hosseini, S.; Kouzmanova, M.; Hołyńska, M.; Tranca, I.; Larkum, A. W.; Shen, J.-R.; Allakhverdiev, S. I., Water-oxidizing complex in Photosystem II: Its structure and relation to manganese-oxide based catalysts. *Coord. Chem. Rev.* **2020,** *409*, 213183.
3. Luber, S.; Rivalta, I.; Umena, Y.; Kawakami, K.; Shen, J.-R.; Kamiya, N.; Brudvig, G. W.; Batista, V. S., S_1-State Model of the O_2-Evolving Complex of Photosystem II. *Biochemistry* **2011,** *50* (29), 6308-6311.
4. Grundmeier, A.; Dau, H., Structural models of the manganese complex of photosystem II and mechanistic implications. *Biochim. Biophys. Acta* **2012,** *1817* (1), 88-105.
5. Cox, N.; Pantazis, D. A.; Lubitz, W., Current Understanding of the Mechanism of Water Oxidation in Photosystem II and Its Relation to XFEL Data. *Annu. Rev. Biochem* **2020,** *89* (1), 795-820.
6. Lionetti, D.; Agapie, T., How calcium affects oxygen formation. *Nature* **2014,** *513* (7519), 495-496.
7. Cox, N.; Retegan, M.; Neese, F.; Pantazis, D. A.; Boussac, A.; Lubitz, W., Electronic structure of the oxygenevolving complex in photosystem II prior to O-O bond formation. *Science* **2014,** *345* (6198), 804-808.
8. Yocum, C. F., The calcium and chloride requirements of the O_2 evolving complex. *Coord. Chem. Rev.* **2008,** *252* (3-4), 296-305.
9. McEvoy, J. P.; Brudvig, G. W., Water-splitting chemistry of photosystem II. *Chem. Rev.* **2006,** *106* (11), 4455-4483.

10. Loll, B.; Kern, J.; Saenger, W.; Zouni, A.; Biesiadka, J., Towards complete cofactor arrangement in the 3.0A° resolution structure of photosystem II. *Nature* **2005,** *438*, 1040-1044.
11. Lohmiller, T.; Cox, N.; Su, J.-H.; Messinger, J.; Lubitz, W., The Basic Properties of the Electronic Structure of the Oxygen-evolving Complex of Photosystem II Are Not Perturbed by Ca^{2+} Removal. *J. Biol. Chem.* **2012,** *287* (29), 24721-24733.
12. Siegbahn, P. E. M., Water oxidation energy diagrams for photosystem II for different protonation states, and the effect of removing calcium. *Phys. Chem. Chem. Phys.* **2014,** *16* (24), 11893-11900.
13. Boussac, A.; Rappaport, F.; Carrier, P.; Verbavatz, J. M.; Gobin, R.; Kirilovsky, D.; Rutherford, A. W.; Sugiura, M., Biosynthetic Ca^{2+}/Sr^{2+} exchange in the photosystem II oxygen-evolving enzyme of Thermosynechococcus elongatus. *J. Biol. Chem.* **2004,** *279* (22), 22809-22819.
14. Beckmann, K.; Ishida, N.; Boussac, A.; Messinger, J., Effects of the Calcium/strontium and chloride/bromide substitution on substrate water exchange rates in photosystem II. *Photosynth. Res.* **2007,** *91* (2-3), 176-176.
15. Cox, N.; Rapatskiy, L.; Su, J.-H.; Pantazis, D. A.; Sugiura, M.; Kulik, L.; Dorlet, P.; Rutherford, A. W.; Neese, F.; Boussac, A.; Lubitz, W.; Messinger, J., Effect of Ca^{2+}/Sr^{2+} Substitution on the Electronic Structure of the Oxygen-Evolving Complex of Photosystem II: A Combined Multifrequency EPR, ^{55}Mn-ENDOR, and DFT Study of the S_2 State. *J. Am. Chem. Soc.* **2011,** *133* (10), 3635-3648.
16. Yachandra, V. K.; Yano, J., Calcium in the oxygen-evolving complex: Structural and mechanistic role determined by X-ray spectroscopy. *J. Photochem. Photobiol., B* **2011,** *104* (1–2), 51-59.
17. Shamsipur, M.; Pashabadi, A., What has biomimicry so far brought on mysterious natural oxygen evolution? *Coord. Chem. Rev.* **2019,** *401*, 213068.
18. Paul, S.; Neese, F.; Pantazis, D. A., Structural models of the biological oxygen-evolving complex: achievements, insights, and challenges for biomimicry. *Green Chemistry* **2017,** *19* (10), 2309-2325.
19. Paul, S.; Cox, N.; Pantazis, D. A., What Can We Learn from a Biomimetic Model of Nature's Oxygen-Evolving Complex? *Inorg. Chem.* **2017,** *56* (7), 3875-3888.
20. Lee, H. B.; Tsui, E. Y.; Agapie, T., A $CaMn_4O_2$ model of the biological oxygen evolving complex: synthesis via cluster expansion on a low symmetry ligand. *Chem. Commun.* **2017,** *53* (51), 6832-6835.
21. Melnic, S.; Shova, S.; Benniston, A. C.; Waddell, P. G., Evolution of manganese-calcium cluster structures based on nitrogen and oxygen donor ligands. *CrystEngComm* **2017**.
22. Arauzo, A.; Bartolomé, E.; Benniston, A. C.; Melnic, S.; Shova, S.; Luzón, J.; Alonso, P. J.; Barra, A.-L.; Bartolomé, J., Slow magnetic relaxation in a dimeric Mn2Ca2 complex enabled by the large Mn(iii) rhombicity. *Dalton Trans.* **2017,** *46* (3), 720-732.
23. Mousazade, Y.; Mohammadi, M. R.; Bagheri, R.; Bikas, R.; Chernev, P.; Song, Z.; Lis, T.; Siczek, M.; Noshiranzadeh, N.; Mebs, S.; Dau, H.; Zaharieva, I.; Najafpour, M. M., A synthetic manganese–calcium cluster similar to the catalyst of Photosystem II: challenges for biomimetic water oxidation. *Dalton Trans.* **2020,** *49* (17), 5597-5605.
24. Chen, C.; Li, Y.; Zhao, G.; Yao, R.; Zhang, C., Natural and Artificial Mn_4Ca Cluster for the Water Splitting Reaction. *ChemSusChem* **2017,** *10* (22), 4403-4408.
25. Koepf, M.; Bergkamp, J. J.; Teillout, A. L.; Llansola-Portoles, M. J.; Kodis, G.; Moore, A. L.; Gust, D.; Moore, T. A., Design of porphyrin-based ligands for the assembly of d-block metal : calcium bimetallic centers. *Dalton Trans.* **2017,** *46* (13), 4199-4208.
26. Alaimo, A. A.; Koumousi, E. S.; Cunha-Silva, L.; McCormick, L. J.; Teat, S. J.; Psycharis, V.; Raptopoulou, C. P.; Mukherjee, S.; Li, C.; Gupta, S. D.; Escuer, A.; Christou,

G.; Stamatatos, T. C., Structural Diversities in Heterometallic Mn–Ca Cluster Chemistry from the Use of Salicylhydroxamic Acid: {$MnIII_4Ca_2$}, {$MnII/III_6Ca_2$}, {$MnIII/IV_8Ca$}, and {$MnIII_8Ca_2$} Complexes with Relevance to Both High- and Low-Valent States of the Oxygen-Evolving Complex. *Inorg. Chem.* **2017,** *56* (17), 10760-10774.
27. Alaimo, A. A.; Alexandropoulos, D. I.; Lampropoulos, C.; Stamatatos, T. C., New insights in Mn–Ca chemistry from the use of oximate-based ligands: {$MnII/III_{22}Ca_2$} and {$MnIV_2Ca_2$} complexes with relevance to both low- and high-valent states of the oxygen-evolving complex. *Polyhedron* **2018,** *149*, 39-44.
28. Chen, C.; Chen, Y.; Yao, R.; Li, Y.; Zhang, C., Artificial Mn_4Ca Clusters with Exchangeable Solvent Molecules Mimicking the Oxygen-Evolving Center in Photosynthesis. *Angew. Chem. Int. Ed.* **2019,** *58* (12), 3939-3942.
29. Tziotzi, T. G.; Andreou, E. K.; Tzanetou, E.; Kalofolias, D. A.; Cutler, D. J.; Weselski, M.; Siczek, M.; Lis, T.; Brechin, E. K.; Milios, C. J., The first amino acid bound manganese–calcium clusters: a {[$MnIII_3Ca]_2$} methylalanine complex, and a [$MnIII_6Ca$] trigonal prism. *Dalton Trans.* **2020,** *49* (30), 10339-10343.
30. Mukherjee, S.; Stull, J. A.; Yano, J.; Stamatatos, T. C.; Pringouri, K.; Stich, T. A.; Abboud, K. A.; Britt, R. D.; Yachandra, V. K.; Christou, G., Synthetic model of the asymmetric [Mn_3CaO_4] cubane core of the oxygen-evolving complex of photosystem II. *PNAS* **2012,** *109* (7), 2257-2262.
31. Zhang, C.; Chen, C.; Dong, H.; Shen, J.-R.; Dau, H.; Zhao, J., A synthetic Mn_4Ca-cluster mimicking the oxygen-evolving center of photosynthesis. *Science* **2015,** *348* (6235), 690-693.
32. Kanady, J. S.; Tsui, E. Y.; Day, M. W.; Agapie, T., A Synthetic Model of the Mn_3Ca Subsite of the Oxygen-Evolving Complex in Photosystem II. *Science* **2011,** *333* (6043), 733-736.
33. Kanady, J. S.; Lin, P.-H.; Carsch, K. M.; Nielsen, R. J.; Takase, M. K.; Goddard, W. A., III; Agapie, T., Toward Models for the Full Oxygen-Evolving Complex of Photosystem II by Ligand Coordination To Lower the Symmetry of the Mn_3CaO_4 Cubane: Demonstration That Electronic Effects Facilitate Binding of a Fifth Metal. *J. Am. Chem. Soc.* **2014,** *136* (41), 14373-14376.
34. Martin-Diaconescu, V.; Gennari, M.; Gerey, B.; Tsui, E.; Kanady, J.; Tran, R.; Pecaut, J.; Maganas, D.; Krewald, V.; Goure, E.; Duboc, C.; Yano, J.; Agapie, T.; Collomb, M.-N.; DeBeer, S., Ca K-Edge XAS as a Probe of Calcium Centers in Complex Systems. *Inorg. Chem.* **2015,** *54* (4), 1283-1292.
35. Gerey, B.; Gennari, M.; Goure, E.; Pecaut, J.; Blackman, A.; Pantazis, D. A.; Neese, F.; Molton, F.; Fortage, J.; Duboc, C.; Collomb, M.-N., Calcium and heterometallic manganese-calcium complexes supported by tripodal pyridine-carboxylate ligands: structural, EPR and theoretical investigations. *Dalton Trans.* **2015,** *44* (28), 12757-12770.
36. Mezei, G.; Zaleski, C. M.; Pecoraro, V. L., Structural and functional evolution of metallacrowns. *Chem. Rev.* **2007,** *107* (11), 4933-5003.
37. Abufarag, A.; Vahrenkamp, H., Zinc Complexes of the Ligand Dipicolylglycine. *Inorg. Chem.* **1995,** *34* (8), 2207-2216.
38. Ménage, S.; Fujii, H.; Hendrich, M. P.; Que Jr., L., Carboxylatoiron(II) Aggregates: A Novel Fe Complex with Threefold Symmetry. *Angew. Chem., Int. Ed. Engl.* **1994,** *33* (15- 16), 1660-1662.
39. Mandal, S. K.; Young, V. G.; Que, L., Polynuclear Carboxylato-Bridged Iron(II) Clusters: Synthesis, Structure, and Host−Guest Chemistry. *Inorg. Chem.* **2000,** *39* (8), 1831-1833.

40. Zhang, Y.-J.; Ma, B.-Q.; Gao, S.; Li, J.-R.; Liu, Q.-D.; Wen, G.-H.; Zhang, X.-X., The first lanthanide-templated molecular wheel containing six copper ions *J. Chem. Soc., Dalton Trans.* **2000,** (14), 2249-2250.
41. Wang, X.; Vittal, J. J., Nature of the Reactants and Influence of Water on the Supramolecular Assembly. *Inorg. Chem.* **2003,** *42* (17), 5135-5142.
42. Lah, M. S.; Pecoraro, V. L., Isolation and characterization of $\{Mn^{II}[Mn^{III}(salicylhydroximate)]_4(acetate)_2(DMF)_6\}$.cntdot.2DMF: an inorganic analog of M^{2+}(12-crown-4). *J. Am. Chem. Soc.* **1989,** *111* (18), 7258-7259.
43. Gibney, B. R.; Wang, H.; Kampf, J. W.; Pecoraro, V. L., Structural Evaluation and Solution Integrity of Alkali Metal Salt Complexes of the Manganese 12-Metallacrown-4 (12-MC-4) Structural Type. *Inorg. Chem.* **1996,** *35* (21), 6184-6193.
44. Dendrinou-Samara, C.; Papadopoulos, A. N.; Malamatari, D. A.; Tarushi, A.; Raptopoulou, C. P.; Terzis, A.; Samaras, E.; Kessissoglou, D. P., Inter-conversion of 15-MC-5 to 12-MC-4 manganese metallacrowns: structure and bioactivity of metallacrowns hosting carboxylato complexes. *J. Inorg. Biochem.* **2005,** *99* (3), 864-875.
45. Koumousi, E. S.; Mukherjee, S.; Beavers, C. M.; Teat, S. J.; Christou, G.; Stamatatos, T. C., Towards models of the oxygen-evolving complex (OEC) of photosystem II: a Mn_4Ca cluster of relevance to low oxidation states of the OEC. *Chem. Commun.* **2011,** *47* (39), 11128-11130.
46. Alaimo, A. A.; Takahashi, D.; Cunha-Silva, L.; Christou, G.; Stamatatos, T. C., Emissive $\{Mn_4^{III}Ca\}$ Clusters with Square Pyramidal Topologies: Syntheses and Structural, Spectroscopic, and Physicochemical Characterization. *Inorg. Chem.* **2015,** *54* (5), 2137-2151.
47. Azar, M. R.; Boron, T. T., III; Lutter, J. C.; Daly, C. I.; Zegalia, K. A.; Nimthong, R.; Ferrence, G. M.; Zeller, M.; Kampf, J. W.; Pecoraro, V. L.; Zaleski, C. M., Controllable Formation of Heterotrimetallic Coordination Compounds: Systematically Incorporating Lanthanide and Alkali Metal Ions into the Manganese 12-Metallacrown-4 Framework. *Inorg. Chem.* **2014,** *53* (3), 1729-1742.
48. Foley, C. M.; Armanious, M. A.; Smihosky, A. M.; Zeller, M.; Zaleski, C. M., Syntheses and Crystal Structures of a Series of Manganese-Lanthanide-Sodium 12-Metallacrown-4 Dimers. *J. Chem. Crystallogr.* **2020**.
49. Shannon, R., Revised effective ionic radii and systematic studies of interatomic distances in halides and chalcogenides. *Acta Crystallographica Section A* **1976,** *32* (5), 751-767.
50. Tsui, E. Y.; Agapie, T., Reduction potentials of heterometallic manganese-oxido cubane complexes modulated by redox-inactive metals. *Proc. Natl. Acad. Sci. USA* **2013,** *110* (25), 10084-10088.
51. Romero, I.; Collomb, M.-N.; Deronzier, A.; Llobet, A.; Perret, E.; Pécaut, J.; Pape, L. L.; Latour, J.-M., A Novel Dimanganese(II) Complex with Two Chloride Bridges. A Two-Electron Oxidation System. *Eur. J. Inorg. Chem.* **2001,** (1), 69-72.
52. Romain, S.; Rich, J.; Sens, C.; Stoll, T.; Benet-Buchholz, J.; Llobet, A.; Rodriguez, M.; Romero, I.; Clerac, R.; Mathoniere, C.; Duboc, C.; Deronzier, A.; Collomb, M.-N., Multireversible Redox Processes in Pentanuclear Bis(Triple-Helical) Manganese Complexes Featuring an Oxo-Centered triangular $\{MnII_2Mn^{III}(\mu_3\text{-}O)\}^{5+}$ or $\{Mn^{II}MnIII_2(\mu_3\text{-}O)\}^{6+}$ Core Wrapped by Two $\{MnII_2(bpp)_3\}^{-}$. *Inorg. Chem.* **2011,** *50* (17), 8427-8436.
53. Gouré, E.; Gerey, B.; Molton, F.; Pécaut, J.; Clérac, R.; Thomas, F.; Fortage, J.; Collomb, M.-N., Seven Reversible Redox Processes in a Self-Assembled Cobalt Pentanuclear Bis(triple-stranded helicate): Structural, Spectroscopic, and Magnetic Characterizations in the $CoICoII_4$, $CoII_5$, and $CoII_3CoIII_2$ Redox States. *Inorg. Chem.* **2020,** *59* (13), 9196-9205.

54. Tsui, E. Y.; Tran, R.; Yano, J.; Agapie, T., Redox-inactive metals modulate the reduction potential in heterometallic manganese-oxido clusters. *Nat. Chem.* **2013,** *5* (4), 293-299.
55. Collomb, M.-N.; Deronzier, A., Manganese Inorganic & Coordination Chemistry. *Encyclopedia of Inorganic Chemistry, 2nd edn., (Ed.: R. B. King), Wiley,* **2005,** *5*, p. 2894-2907.
56. Collomb, M.-N.; Mantel, C.; Romain, S.; Duboc, C.; Leprêtre, J.-C.; Pécaut, J.; Deronzier, A., Redox-Induced μ-Acetato and μ-Oxo Core Interconversions in Dinuclear Manganese Tris(2-methylpyridyl)amine (tpa) Complexes: Isolation and Characterization of $[Mn_2^{III}(\mu\text{-}O)(\mu\text{-}O_2CCH_3)(tpa)_2]^{3+}$. *Eur. J. Inorg. Chem.* **2007**, 3179-3187.
57. Duboc, C.; Collomb, M.-N.; Pécaut, J.; Deronzier, A.; Neese, F., Definition of Magneto-Structural Correlations for the Mn^{II} Ion. *Chem. Eur. J.* **2008,** *14*, 6498-6509.
58. Mantel, C.; Baffert, C.; Romero, I.; Deronzier, A.; Pecaut, J.; Collomb, M. N.; Duboc, C., Structural characterization and electronic properties determination by high-field and high-frequency EPR of a series of five-coordinated Mn(II) complexes. *Inorg. Chem.* **2004,** *43* (20), 6455-6463.
59. Romero, I.; Dubois, L.; Collomb, M.-N.; Deronzier, A.; Latour, J.-M.; Pécaut, J., A Dinuclear Manganese(II) Complex with the $\{Mn_2(\mu\text{-}O_2CCH_3)_3\}^+$ Core: Synthesis, Structure, Characterization, Electroinduced Transformation, and Catalase-like Activity. *Inorg. Chem.* **2002,** (41), 1795-1806.
60. Collomb, M.-N.; Deronzier, A., Electro- and Photoinduced Formation and Transformation of Oxido-Bridged Multinuclear Mn Complexes. *Eur. J. Inorg. Chem.* **2009**, 2025-2046.
61. Baffert, C.; Collomb, M. N.; Deronzier, A.; Kjaergaard-Knudsen, S.; Latour, J. M.; Lund, K. H.; McKenzie, C. J.; Mortensen, M.; Nielsen, L.; Thorup, N., Biologically relevant mono- and di-nuclear manganese II/III/IV complexes of mononegative pentadentate ligands. *Dalton Trans.* **2003,** (9), 1765-1772.
62. de Muro, I. G.; Insausti, M.; Lezama, L.; Urtiaga, M. K.; Arriortua, M. I.; Rojo, T., Study of the [CaM($C_3H_2O_4$)(2)(H_2O)(4)]center dot nH_2O [M = Mn, Fe or Co (n=0) and Ni (n=2)] systems: synthesis, structure, spectroscopic and magnetic properties. *J. Chem. Soc., Dalton Trans.* **2000,** (19), 3360-3364.
63. Benniston, A. C.; Melnic, S.; Turta, C.; Arauzo, A. B.; Bartolome, J.; Bartotome, E.; Harrington, R. W.; Probert, M. R., Preparation and properties of a calcium(II)-based molecular chain decorated with manganese(II) butterfly-like complexes. *Dalton Trans.* **2014,** *43* (35), 13349-13357.
64. Li, N.; Wang, M.; Ma, C.-B.; Hu, M.-Q.; Zhou, R.-W.; Chen, H.; Chen, C.-N., Synthesis and characterization of a new 2D trimetallic Mn/Ca/Na complex. *Inorg. Chem. Commun.* **2010,** *13* (6), 730-732.
65. Kotzabasaki, V.; Siczek, M.; Lis, T.; Milios, C. J., The first heterometallic Mn-Ca cluster containing exclusively Mn(III) centers. *Inorg. Chem. Commun.* **2011,** *14* (1), 213-216.
66. Park, Y. J.; Ziller, J. W.; Borovik, A. S., The Effects of Redox-Inactive Metal Ions on the Activation of Dioxygen: Isolation and Characterization of a Heterobimetallic Complex Containing a Mn^{III}-(mu-OH)-Ca^{II} Core. *J. Am. Chem. Soc.* **2011,** *133* (24), 9258-9261.
67. Cook, S. A.; Borovik, A. S., Molecular Designs for Controlling the Local Environments around Metal Ions. *Acc. Chem. Res.* **2015,** *48* (8), 2407-2414.
68. Park, Y. J.; Cook, S. A.; Sickerman, N. S.; Sano, Y.; Ziller, J. W.; Borovik, A. S., Heterobimetallic complexes with M^{III}-(mu-OH)-M^{II} cores (M^{III} = Fe, Mn, Ga; M^{II} = Ca, Sr, and Ba): structural, kinetic, and redox properties. *Chem. Sci.* **2013,** *4* (2), 717-726.

69. Jerzykiewicz, L. B.; Utko, J.; Duczmal, M.; Sobota, P., Syntheses, structure, and properties of a manganese-calcium cluster containing a Mn4Ca2 core. *Dalton Trans.* **2007,** (8), 825-826.
70. Fuller, R. O.; Koutsantonis, G. A.; Lozic, I.; Ogden, M. I.; Skelton, B. W., Manganese-calcium clusters supported by calixarenes. *Dalton Trans.* **2015,** *44* (5), 2132-2137.
71. Hewitt, I. J.; Tang, J. K.; Madhu, N. T.; Clérac, R.; Buth, G.; Anson, C. E.; Powell, A. K., A series of new structural models for the OEC in photosystem II. *Chem. Commun.* **2006,** (25), 2650-2652.
72. Nayak, S.; Nayek, H. P.; Dehnen, S.; Powell, A. K.; Reedijk, J., Trigonal propeller-shaped [Mn_3(III)M(II)Na] complexes (M = Mn, Ca): structural and functional models for the dioxygen evolving centre of PSII. *Dalton Trans.* **2011,** *40* (12), 2699-2702.
73. Mishra, A.; Wernsdorfer, W.; Abboud, K. A.; Christou, G., The first high oxidation state manganese-calcium cluster: relevance to the water oxidizing complex of photosynthesis. *Chem. Commun.* **2005,** (1), 54-56.
74. Mishra, A.; Yano, J.; Pushkar, Y.; Yachandra, V. K.; Abboud, K. A.; Christou, G., Heteronuclear Mn-Ca/Sr complexes, and Ca/Sr EXAFS spectral comparisons with the oxygen-evolving complex of photosystem II. *Chem. Commun.* **2007,** (15), 1538-1540.
75. Chen, C.; Zhang, C.; Dong, H.; Zhao, J., Artificial synthetic MnIVCa-oxido complexes mimic the oxygen-evolving complex in photosystem II. *Dalton Trans.* **2015,** *44* (10), 4431-4435.
76. Chen, C.; Zhang, C.; Dong, H.; Zhao, J., A synthetic model for the oxygen-evolving complex in Sr2+-containing photosystem II. *Chem. Commun.* **2014,** *50* (66), 9263-9265.
77. Escriche-Tur, L.; Jover, J.; Font-Bardia, M.; Aullón, G.; Corbella, M., Magnetic Behavior of Heterometallic Wheels Having a $[MnIV_6M_2O_9]^{10+}$ Core with M = Ca^{2+} and Sr^{2+}. *Inorg. Chem.* **2015,** *54* (24), 11596-11605.

For Table of Contents Only

Rare examples of homo- and heteronuclear μ-carboxylato-bridged metallacrown complexes of the type 12-MC-3 and 8-MC-4 were isolated from the hexadentate tripodal ligands incorporating two carboxylate functions. The heteronuclear complexes also join the small family of Mn-Ca complexes and even rarer Mn-Sr complexes as models of the OEC of photosystem II. The 12-MC-3 tetranuclear structures are stable in solution, both in the initial oxidation state, $\mathbf{Mn^{II}_3M}$, as well as in the three-electrons oxidized state, $\mathbf{Mn^{III}_3M}$.